Summer 2021

Expression, Purification and Characterization of the Human Cytochrome P450 Enzyme 4x1 (CYP4X1) Using Substrate Binding Affinity, Metabolic Assays and Protein Crystallization

Olusegun Adeolu Idowu
Missouri State University, Olusegun291@missouristate.edu

EXPRESSION, PURIFICATION AND CHARACTERIZATION OF THE HUMAN CYTOCHROME P450 ENZYME 4X1 (CYP4X1) USING SUBSTRATE BINDING AFFINITY, METABOLIC ASSAYS AND PROTEIN CRYSTALLIZATION

A Master's Thesis

Presented to

The Graduate College of

Missouri State University

In Partial Fulfillment

Of the Requirements for the Degree

Master of Science, Chemistry

By

Olusegun Adeolu Idowu

July 2021

EXPRESSION, PURIFICATION AND CHARACTERIZATION OF THE HUMAN CYTOCHROME P450 ENZYME 4X1 (CYP4X1) USING SUBSTRATE BINDING AFFINITY, METABOLIC ASSAYS AND PROTEIN CRYSTALLIZATION

Chemistry

Missouri State University, July 2021

Master of Science

Olusegun Adeolu Idowu

ABSTRACT

The human cytochrome P450 enzyme 4X1 (*CYP4X1*) is among the "orphan" cytochrome P450 meaning there is much unknown about its structure, biological function, and regulation in literature study. Scientific work on this protein has primarily been on identifying its physiological functions and expression sites. A recent study found 2 substrates (arachidonic acid and anandamide) catalyzed by the enzyme. Expression in humans appears to be primarily in the brain, prostate, lungs, and neurovascular systems and research has linked the protein as a potential chemotherapy target in brain cancer. So far, only a few inhibitors have been identified. The goal of this research is to characterize CYP4X1. The first step is to express the protein in *E. coli JM109* cell using either the *pCW* or *pET28a* vector. Protein expression attempts indicated that *pET28a* vector in *JM 109* cells produced a better yield overall. Protein purification was obtained using cobalt and nickel affinity chromatography made possible by a 6-residue histidine tag affixed to the protein's C-terminal following expression. Protein purification is followed by SDS-PAGE to ascertain purity. Binding affinity assays were obtained for the two previously published substrates, arachidonic acid, and anandamide. Additional compounds that could be ligands based on their structural similarity to arachidonic were also assayed. Purified protein was concentrated and screened with a commercial crystal screen and a crystal hit has been identified with further optimization required.

KEYWORDS: orphan cytochrome P450, protein expression, chromatographic purification, binding affinity assays, protein crystallization

EXPRESSION, PURIFICATION AND CHARACTERIZATION OF THE HUMAN CYTOCHROME P450 ENZYME 4X1 (CYP4X1) USING SUBSTRATE BINDING AFFINITY, METABOLIC ASSAYS AND PROTEIN CRYSTALLIZATION

By

Olusegun Adeolu Idowu

A Master's Thesis
Submitted to the Graduate College
Of Missouri State University
In Partial Fulfillment of the Requirements
For the Degree of Master of Science, Chemistry

July 2021

Approved:

Natasha DeVore, Ph. D., Thesis Committee Chair

Gary Meints, Ph. D., Committee Member

Gautam Bhattacharyya, Ph.D., Committee Member

Christopher Lupfer, Ph.D., Committee Member

Julie Masterson, Ph.D., Dean of the Graduate College

ACKNOWLEDGEMENTS

I want to deeply thank Dr Natasha DeVore for her unrelenting support, patience, tutelage, and peaceful demeanor for the entire stretch of this project. She's indeed a superb human and honorable supervisor. I would also like to acknowledge my research committee members Dr Gary Meints, Dr Gautam Bhattacharyya, and Dr Christopher Lupfer for honoring and supporting this cause with their valuable time and service.

My honorable mention goes to my research colleagues Brenda Wekesa, Mehwish Khokhar Cody Turner, and friends Polycarp Ofoegbu, Lukio Owuocha, Seth Adu-Amankrah, Ademola Odusanya, Chideraa Nwachukwu and Adedamola Opalade for the mentoring sessions over the past 2 years. It was indeed an honor helping with each other's mental health in graduate school. What a journey it has been.

I dedicate this thesis to God almighty, my parents and siblings, my jewels of inestimable value and immense source of encouragement. I love you all.

TABLE OF CONTENTS

LIST OF TABLES

LIST OF FIGURES

CHAPTER 1 - INTRODUCTION

1.1 Cytochrome P450

Cytochromes P450 depicted in Figure 1 is a family of enzymes that have heme as a cofactor and function as monooxygenases. Monooxygenases are enzymes that catalyzes oxidation reactions by adding one atom of oxygen to a substrate, typically as a hydroxyl, through oxidation reactions that give water, $NADP^+$ and hydroxyl of the organic substrate as the products.

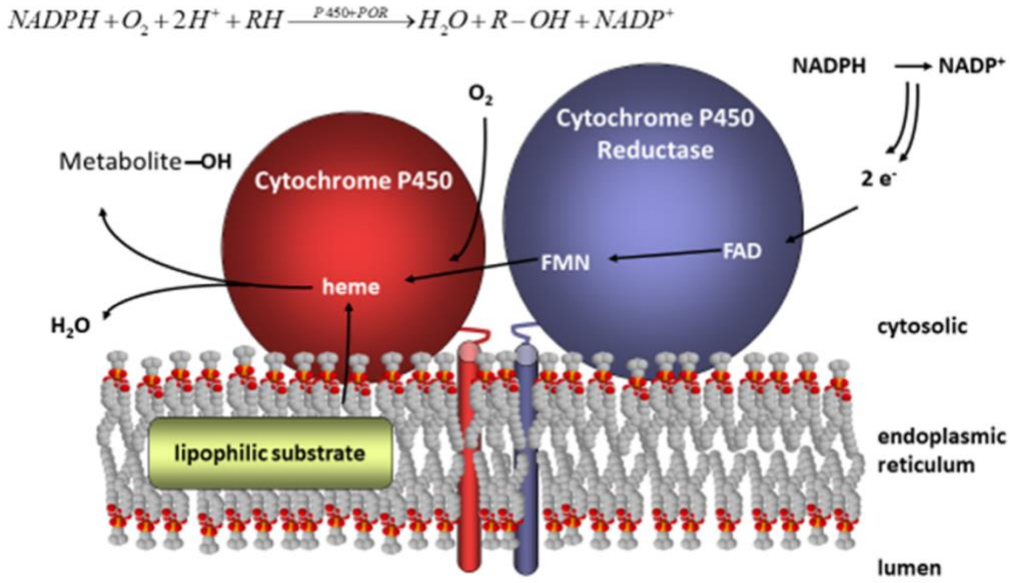

Figure 1: Cartoon depiction of Cytochrome P450 catalytic activity. This reproduced image was made by Natasha DeVore Ph.D., BY CC-SA 4.0, image not modified.

Cytochrome P450 (CYP450) catalytic activity is a membrane bound oxidation of numerous biologically active substrates in a stepwise series of electron transfer reaction starting with nicotinamide adenine dinucleotide phosphate (NADPH). CYP450 requires an additional redox partner in form of CYP450 reductase (POR) that aids in the electron transfer process by

accepting and transferring two electrons that makes the actual CYP450 enzyme catalytically active. (Waskell & Kim, 2015). There is also the needed requirement of both atomic oxygen and NADPH to effect a reaction. NADPH transfers single electrons via hydride ions to flavin adenine dinucleotide (FAD) and then to flavin mononucleotide (FMN). This electron is then used in the conversion of a lipophilic substrate to a hydroxy metabolite and water as by product in endoplasmic reticulum. (Waskell & Kim, 2015).

In humans, the cytochrome P450 enzymes are mainly located in the liver and are membrane-associated proteins found in the inner membranes of mitochondria or the endoplasmic reticulum. Nonetheless, the cytochrome subfamilies, CYP4A, CYP4B, CYP4F, CYP4V, CYP4X, and CYP4Z, are present in most body tissues. (Kumar, 2015).

Cytochrome P450s are involved in the oxidation of fatty acids, steroids, xenobiotics, and the synthesis and breakdown of hormones (Hsu, Savas, Griffin & Johnson, 2007). The cytochrome P450 family is also involved in the removal of xenobiotics, different components of drugs and environmental chemicals, clearance of vitamins, and oxidation of eicosanoids (Stark & Guengerich, 2007). CYP450 may also have a role in immune responses through metabolic modification and regulating eicosanoid concentrations during inflammation (Kalsotra & Strobel, 2006).

There are 54 other cytochrome P450s found in humans**.** However, not all functions of each specific cytochrome P450 are known, Including cytochrome P450 enzyme 4X1 (CYP4X1). CYP4X1 is currently classified as an orphan cytochrome P450, meaning there is still a lot unknown about its structure and function. Only limited studies have been conducted with purified CYP4X1 enzyme. Thus, the expression, purification, and characterization of the CYP4X1 enzyme is our goal to understand the biological role of CYP4X1 better. The

characterization of purified CYP4X1 can be carried out using binding affinity and metabolic assays.

1.2 Literature Review of Enzymatic Function (CYP4X1)

CYP4X1 gene is expressed in the brain (Kharkwal et al., 2017). The CYP4X1 protein on the other hand is present in various tissues in the human body, including the skeletal muscles, trachea, and aorta. (Al-Anizy et al., 2006; Stark, Dostalek & Guengerich, 2008).

Indeed, an original study conducted by Bylund, Zhang & Harder, (2002) first identified a unique CYP450 isoform with localization in the brain. This novel cytochrome was identified from orthologous *c*DNA cloning via reverse transcription-PCR from brain samples of rats. This was the first time the protein was elucidated, and the deduced amino acid sequence exhibited amino acid identity of around 41% - 51% with that of members of the rat CYP4 subfamilies (Bylund, Zhang & Harder, 2002).

The study conducted by Bylund, Zhang & Harder, (2002) used the northern blot to show that the isoform CYP4X1 is highly expressed in the brain. In situ hybridization indicated that it was mainly expressed in different brain regions, such as the cortex, hippocampus, cerebellum, and brain stem, an indication that it may be involved in critical physiological processes (Bylund et al., 2002).

Bylund, Zhang & Harder, (2002) study referenced that CYP4 family is known to be mainly involved in omega hydroxylation of fatty acids like. Also, a more recent evolutionary relationship study by Kirschian & Wilson (2012) determined for CYP4 subfamilies hypothesized that the CYP4X1 is specialized in the metabolism of long-chain fatty acids (e.g., arachidonic acid). The enzyme was identified from EST database as a member of the CYP4X and the human isoform was ultimately designated as CYP4X1 (Bylund, Zhang & Harder, 2002). The human

CYP4X1 gene is found within the P450 ABXZ gene cluster on the first chromosome and is comprised of 509 amino acids. However, the functions of the CYP4X1 cytochrome are mostly unknown, and as such, it is referred to as an 'orphan' cytochrome. (Bylund, Zhang & Harder, 2002).

Similarly, Al-Anizy et al. (2006) showed that the CYP4X1 was principally expressed in the brain and aorta of a mouse model. This was accomplished by using cDNA of the mouse via cloned brain RNA sequence (94% identity); to detect antibodies specifically developed for CYP4X1. The study used the northern blotting technique by using antibodies against modified nucleosides to establish that CYP4XI was expressed in the brain.

Different studies that have been conducted have shown that CYP4X1 might be involved in tumorigenesis, as the expression in cancer cells has been noted to be high (Al-Anizy et al., 2006). Murray, Patimalla, Stewart, Miller & Heys, (2010) conducted a study on the expression of the P450 system in breast cancer cells and their influence on tumor development. In the study, a tissue microarray containing 170 breast cancers was immuno-stained to test out 21 P450 antibodies (CYP4X1 inclusive) via histochemistry. Histochemistry is a biochemical technique that enables the identification of pivotal structures in tissues when stained and viewed under the microscope. The degree of immuno-stained tissues via the distribution of chemical components was determined and used to show the varying levels of CYP450 expressions. The results showed that the cytochrome P450 expression was high, and the levels varied within the subfamilies. Overall, the study by Murray, Patimalla, Stewart, Miller & Heys, (2010) showed that the strongest immunopositivity for breast cancer were highest in percentage at 50.8% for CYP4X1. Figures indicate that CYP variants are actively involved in the metabolism of anticancer drugs targeted for breast cancer. Therefore, the study concluded that the expression of the

monooxygenase enzymes (CYP450s) in the cancer cells was high, which could potentially be tied to down regulation by metabolizing a therapeutic drug that might help target cancer (Hsu, Savas, Griffin & Johnson, 2007).

In another study, Wang et al. (2018) noted that CYP4XI might be involved in human glioma vasculature. The experiment tested the ability of a novel flavonoid 2'-O-Methylhelichrysetin (CH625) to inhibit CYP4XI in tumor-associated macrophages (TAM). Their study showed that CH625 inhibition of CYP4XI caused vasculature normalization leading to improved survival of glioblastoma in rats. Furthermore, the findings indicated that the inhibition by CH625 occurred through the downregulation of vascular endothelial growth factor (VEGF) derived from Tumor-associated macrophages (Wang et al., 2018). Also, the cannabinoid receptors type 11 (CB2) helped in the expression of specific tumor growth factor and activated epidermal growth factor receptor (EGFR) and downstream signal transducer and activator of transcription 3 (STAT3), which are vital in tumor therapy (Wang et al., 2018). In vitro, TAM polarization increased T-cell proliferation and the migration of pericytes, reduced the production of VEGF and transforming growth factor beta (TGF-β), and downregulated the expression of cannabinoid receptors and EGFR (Wang et al., 2018). However, the overexpression of the CYP4X1 and the STAT3 led to the reversal of these effects that were noted after the polarization of TAM, an indication that CYP4X1 is involved in the normalization of the glioma vasculature (Wang et al., 2018). Inhibition of the CYP4X1 by the flavonoid CH625 also led to the delayed growth and prolonged survival of the affected rats.

In an earlier study, Carmeliet & Jain, (2011) showed that the proliferation and movement of endothelial cells led to the production of immature tumor vessels with low perfusion and

oxygenation thereby inhibiting the survival of glioblastoma cells. This research by Wang et al. (2018) shows promise for the clinical use of inhibitors for CYP4X1.

In another study, Stark, Dostalek & Guengerich (2008) determined the expression in mammalian cells and purification of the CYP4X1 in bacteria. The real-time PCR analysis indicated the protein expression in mRNA in extrahepatic tissues, liver, heart, prostate, breast, and human brain structures such as the amygdala, basal ganglia, and cerebellum (Stark, Dostalek & Guengerich, 2008). The substrate used in the experiment was anandamide. A quantitative Polymerase Chain Reaction was used to indicate the cytochrome levels in mRNA of the brain. The results showed that the levels of CYP4X1 expression were high in the brain (Stark, Dostalek & Guengerich, 2008). The researchers concluded that the CYP4X1 gene might have a role in the signaling of the brain, cardiovascular functions, and mediation of signaling in the neurological and immune systems due to the high expression in the amygdala and the distribution patterns.

The expression patterns of the CYP4X1 gene in blood vessels and specific brain regions might indicate that it has a neurovascular role (Al-Anizy et al., 2006). The neurovascular function may be related to the metabolism of arachidonic acid, which is involved in regulating cerebral blood flow (Davis, Liu, & Alkayed, 2017). Arachidonic acid is an essential fatty acid involved in the mediation of inflammation during immune system responses (Tallima & El Ridi, 2018). It has also been noted to have a role in other physiological processes, including mitogenesis, activation of calcium ion-dependent potassium ion channels in cells, vasodilation, and regulating the blood pressure and cellular levels of ions (Stark, Dostalek & Guengerich, 2008).

Derivatives of arachidonic acid such as anandamide and eicosanoids have often been implicated in physiological processes such as mediation of cell signaling, development of

immune reactions, and cardiovascular functions. Cytochrome P450 enzymes can also modify these derivatives (Stark, Dostalek & Guengerich, 2008). The anandamide binds to a cannabinoid receptor as it is an endogenous cannabinoid receptor ligand (Stark, Dostalek & Guengerich, 2008). At high concentrations, studies have shown that the anandamide is an agonist of vanilloid receptor-1 mediated functional responses such as the vasodilation of small arteries and the development of inflammatory and acute pain signals (Stark, Dostalek & Guengerich, 2008; Ross, 2003).

Binding assays can be used to determine the substrate affinity of a ligand for a protein. The binding affinity of arachidonic acid and anandamide to CYP4X1 is not known. Different assays have explored the binding affinities of various fatty acids to other membrane bound catalytic enzymes.

Different studies have been carried out to understand the structure and function of CYP4X1. For instance, Kumar (2015) developed a homology model using Modeller 9v8 to identify the binding site of CYP4X1 and demonstrate the topology of the active site. Different programs were used to assess the protein's energy stability, its geometrical errors, and structural validation. The model was then used for molecular docking of the fatty acid and its derivative; namely arachidonic acid and anandamide respectively (Kumar, 2015).

The results obtained by Kumar (2015) suggests that various amino acid residues, including threonine 312, phenylalanine 491, alanine 126, serine 251, and asparagine 319, were involved in the interaction of arachidonic with the CYP4X1. Also, they showed that the interaction of arachidonic acid derivative, anandamide, was aided by amino acid residues such as leucine 315, serine 251, alanine 126, phenylalanine 491, and proline 118 (Kumar, 2015). These

amino acid residues influence the Cytochrome P450 system's catalytic activity and can be used as candidates for mutagenesis to further test the importance of the residues (Kumar, 2015).

Furthermore, Kumar (2015) studied arachidonic acid and anandamide using the Lipinski rule drug-likeness test to demonstrate their effectiveness as orally active compounds. The Lipinski rule is an industry adopted rule of thumb that entails 5 medicinal chemistry criteria required during drug discovery, research, and testing. These 5 parameters range from molecular weights, partition coefficient, hydrogen bond acceptors and donors etc. Kumar (2015) concluded that the binding of arachidonic acid to the cytochrome P450 system required the action of key amino residues on the CYP4X1 polypeptide sequence. However, the acid's binding was stronger at −7.76kcal/mol than that of its derivative at −5.76 kcal/mol. Both arachidonic acid and anandamide predicted anti-carcinogenic activity based on reported biological spectrum data and the potential of being used as a drug target for cancer therapy (Kumar, 2015). Kumar (2015) study was useful in indicating the roles that the CYP4X1 system might be involved in and provided a model of its structure.

Similarly, the review by Davis, Liu & Alkayed (2017) showed that CYP4X1 might have a role in the maintenance of neurovascular homeostasis and cell signaling. Stark, Dostalek & Guengerich (2008) indicates that CYP4X1 may be involved in cardiovascular functions were further supported by a study by Carver, Lourim, Tryba, & Harder, (2014). Carver, Lourim, Tryba, & Harder, (2014) demonstrated that there is a circadian regulation of the expression of CYP4X1 gene. However, the overall cause of circadian changes in blood flow is unknown (Carver, Lourim, Tryba, & Harder, 2014). CYP4X1 oxidizes arachidonic acid in its expression sites (brain and vascular systems) to yield epoxyeicosatrienoic acids (EETs) (Stark, Dostalek & Guengerich, 2008). EETs induce an associated blood flow increase via vasodilation (Carver,

Lourim, Tryba, & Harder, 2014). Given the role of CYP4X1 in the cardiovascular system, Carver, Lourim, Tryba, & Harder, (2014) study suggests that the presence of arachidonic acid may influence circadian changes in blood flow by testing if the EETs obtained from the oxidation of arachidonic acid vary in a circadian manner. Carver, Lourim, Tryba, & Harder, (2014) experiments were inconclusive and requires further studies. Also, it is noteworthy that Snider, Kornilov, Kent, & Hollenberg, (2007) demonstrated that cytochrome P450s had negligible action in oxidizing anandamide.

Kharkwal et al., (2017) carried out a study to determine the effects of CYP4X1 in the metabolism of energy and the impacts of the bodyweight of mice. The study investigated whether the action of the CYP4X1 influences the endocannabinoid signaling systems that affect energy metabolism and appetite. The endocannabinoid system is an intercellular signaling system with a role in the homeostasis of energy by matching the intake of calories and energy use (Cristino, Becker, & DiMarzo, 2014).

In a Kharkwal et al. (2017) study, transgenic knockout mice were developed. Their total mRNA in different organs like the brain, heart, skin, kidney, colon, lungs, aorta, and liver were quantified through PCR and spectrophotometry. The body weight effects of food intake on mice were recorded and evaluated after a standard rodent and high fat diet was provided for some weeks (Kharkwal et al., 2017). The mice were then monitored comprehensively and tested for blood and glucose tolerance. Also, the net weight of the epididymal fat pads of the knockout and control mice were determined (Kharkwal et al., 2017). The results showed that CYP4X1 knockout mice had more bodyweight than the control mice with similar genetic backgrounds (Kharkwal et al., 2017). Also, the knockout mice had more intra-abdominal fat deposits and enlarged adipocytes.

The results obtained by Kharkwal et al. (2017) also showed differences in the respiratory exchange ratio (RER) in the mice. RER is basically the volume ratio between the carbon dioxide produced and the oxygen used by the body. Vco_2/Vo_2 can be used in estimating which fuel (carbohydrate or fat) is being metabolized during rest or mild aerobic activities. This is a biomarker for respiratory fitness and the amount of adipocyte present. The knockout mice had a reduced RER than the control mice (Kharkwal et al., 2017). The low exchange ratio in mice with high adiposity levels was consistent with the results of studies showing that increased adiposity is associated with a high degree of fat oxidation that negatively affects the respiration system. Kharkwal et al. (2017) concluded that CYP4X1 has a role in regulating fat metabolism and the influence of appetite.

1.3 Significance of the Study

CYP4X1 is an orphan cytochrome as its functions in endogenous and exogenous metabolism have not been entirely documented. Only limited studies have been conducted with purified CYP4X1 enzyme. The location of the gene and its variants in the human genome are well established. There is also some evidence that CYP4X1 may be involved in physiological roles such as inflammation. However, significant knowledge about the exact placement of CYP4X1's role in these processes is unknown. The CYP4X1 gene has been expressed using real time PCR analysis in different organs in the human body, such as the brain, heart, prostate skin, breast, and liver (Stark, Dostalek & Guengerich, 2008).

Although arachidonic acid and anandamide have both been identified as substrates, the substrate turnover is not at a rate consistent for a typical cytochrome P450 with endogenous substrates (high nM or very low μM K_m range). Studies have shown that the binding of identified

substrates is aided by various amino acids that influence their catalytic activity (Kumar 2015). Both arachidonic acid and anandamide are involved in multiple physiological functions, including mitogenesis, vasodilation, blood pressure regulation, and cellular ion levels. (Tallima & El Ridi, 2018; Snider, Kornilov, Kent & Hollenberg, 2007). Since it is involved in the oxidation of arachidonic acid, the cytochrome P450 system is thought to have a direct role in these physiological processes. However, it is also possible that CYP4X1's involvement is due to the metabolism of an alternative yet unidentified substrate.

1.4 Experimental Design

This study involved the expression, purification, and characterization of CYP4X1 to investigate its binding affinity with ligands. This was accomplished by adopting similar best practices from advances and failures on recombinant protein expression in Escherichia coli by (Rosano & Ceccarelli, 2014).

A bacterial plasmid (pET28a) and cloned vector (pCW) was used to express the gene in *Escherichia coli* bacteria JM109 cells. CYP4X1 purification was conducted using Ni-NTA (nickel beads) and cobalt affinity column chromatography, a technique made possible by a 6-residue histidine tag cloned in sequence with the CYP4X1 gene in the plasmid.

This step was followed by Sodium Dodecyl Sulfate Polyacrylamide Gel Electrophoresis (SDS–PAGE) to ascertain protein purity following the purification. The technique entailed using Coomassie blue stain to detect bands containing as low as 100 nanograms of protein rapidly (Raynal, Lenormand, Baron, Hoos & England, 2014). UV-VIS spectrophotometry was used to confirm the purity and to quantify the concentration of CYP4X1 based on the absorbance of the

heme which is specific for that obtained CYP4X1 (Raynal, Lenormand, Baron, Hoos & England, 2014). UV-VIS spectrophotometry is a useful approach for detecting non-protein contaminants.

Ligand binding affinity assay tests with purified CYP4X1 to further characterize the two known substrates and potentially identify other substrates was keenly pursued. Trying out other potential substrate. A more recent study by Pal et al. (2020) for example revealed that the binding affinity of eicosapentaenoic acid and docosahexaenoic acid could be shown by competing for residency with membrane phospholipids (Pal et al., 2020). And perhaps proteins.

Lastly, a crystal screen is performed to determine the crystallization condition of CYP4X1 after the protein optimally purified. The method was designed to provide a highly effective and rapid screening for biological molecules (Wooh, Kidd, Martin & Kobe, 2003). The screens have helped find the initial crystallization conditions for more than 1,000 proteins, peptides, oligonucleotides, and small molecules (Wooh, Kidd, Martin & Kobe, 2003). It uses the features of a sparse matrix screen that effectively sample polymers, salts, pH, and organics.

CHAPTER 2 - MATERIALS AND METHODS

Proteins are ubiquitous in living systems and play diverse and pivotal roles that is essential to sustain life. Yet, proteins especially those associated with membranes are delicate, finicky, and quite painstaking to elucidate in research which in turn affects obtainable yield. In this project, both the materials and methods used were established and adopted from published literature (DeVore et al., 2011). The methodology was optimized during multiple expression attempts and purification trials. The protocols leading to CYP4X1 characterization followed a sequential method illustrated in Figure 2 and as follows; cell transformation, protein expression, cell harvest and lysis, protein extraction via proprietary detergent, purification using cobalt, nickel-nitriloacetic acid (Ni-NTA), carboxymethyl (CM) and Diethylaminomethyl (DEAE) beads, assertion of protein purity via SDS-PAGE and characterization using ligand binding assays.

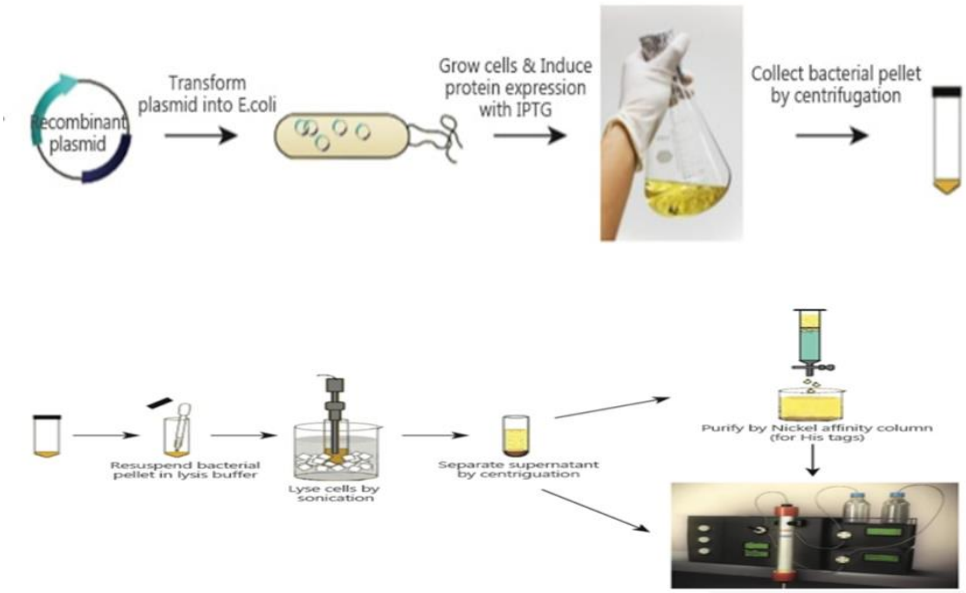

Figure 2. Illustration of expression and purification of CYP4X1. Reproduced from website <https://www.profacgen.com/recombinant-protein-expression-in-ecoli.htm (Accessed 6/22/2021). Images not modified.

Purified protein was also used to screen for crystallization condition for CYP4X1. Thus, in this chapter, the steps and associated material used were discussed in detail.

2.1 Buffer Preparation

Buffers are solutions specially prepared to prevent pH imbalance that could adversely affect functionality of an active protein. The buffers and the recipe used to make them are listed in Table 1.

Table 1: Buffers used for affinity chromatography and ion exchange chromatography.

Buffer Name	Tris Buffer (mM)	Glycerol (mL)	Water (mL)	NaCl (mM)	Imidazole (mM)
Resuspension Buffer	500	50	200	300	N/A
Ni-NTA Wash Buffer	50	50	400	50	10
Ni-NTA Elution Buffer	100	50	400	50	100
Ion Exchange Wash Buffer	50	50	425	N/A	N/A
Ion Exchange Elution Buffer	100	50	400	500	N/A

2.2 Growth Media Preparation

Growth media is prepared prior to the start of protein expression of desired cellular protein. This serves as a source of nutrient for the increase and maintenance of the recombinant *Escherichia Coli* strain. The creation of optimal growth environment needed by bacterial cells during replication is principal to successful protein expression.

2.2.1 Lysogenic broth (LB Media). 1g tryptone, 1 g sodium chloride, 0.5 g yeast extract, 4ml glycerol. The reagents are added into a 150 ml conical flask and partially dissolved with 100ml of water. The resulting solution is covered in aluminum foil and earmarked at the top with

autoclave tape. LB media is autoclaved for 15 minutes at 15 psi and 121-124°C for sterility. Lysogenic broth was used as growth medium for inoculating starter culture.

2.2.2 Terrific broth (TB Media). 50.8g terrific broth powder, 4ml glycerol, 900 ml water to make 1 Liter of terrific broth in a 2-litre conical flask. The broth was autoclaved after mixing components together. Terrific broth was used for cell growth scale up. The medium is suitable for both selective and non-selective cultivation of *E. coli* strains for cloning and higher density yield production of recombinant proteins. As is the case for the method used, selective cultivation is possible when appropriate antibiotics are added to prevent the growth of other microbes.

2.3 Cell Transformation

The CYP4X1 gene carries the encoded instruction that is translated into the desired protein required for characterization. To express CYP4X1 gene into a functional heme protein of *E. coli* JM109 cells, it starts with bacterial cell transformation using heat shock technique. Cell transformation via heat shock enables cell exposure to sudden temperature increase which creates an osmotic pressure difference that induces the formation of pores favorable for the uptake of DNA plasmid or cloned vector. Attenuated *E. coli* JM109 cell strain stored in glycerol at -80°C is placed on an ice bed to thaw. One microliter of purchased plasmid (pET28a) or cloned vector (pCW) carrying the gene that encodes for CYP4X1 protein is aliquot into thawed *E. coli* JM109 cells. The vector and bacteria cells were mixed in an Eppendorf tube and the resultant mixture was placed on ice for 30 minutes. The Eppendorf tube mixture is removed and concurrently placed in 37°C water for 35 seconds. The tube content was aliquot into culture plates containing agar using a micropipette. Then, silica beads were used to spread content across

the entire culture plate. For optimal bacterial growth, the culture plate is placed in an incubator overnight at 37°C.

2.4 Protein Expression

Protein expression in this research was achieved via pET28a plasmid and cloned vector (pCW). To do this, 10 ul of glycerol stock or a single colony of transformed JM109 cells is picked with a micropipette and inoculated into 100ml of autoclaved lysogenic broth (LB media). This is followed by the addition of 100 ul of 50mg/ml antibiotic stock (kanamycin sulfate or ampicillin) to LB media; The antibiotic stock helps prevent the growth of unwanted microbes and ensures that only transformed JM109 cells grow. The *E. coli* immunity to the applied antibiotic has been encoded as information (nucleotide sequence) during gene construct.
The resulting mixture (starter culture) is placed in a shaking incubator all night at 180 rpm and 37°C. An observation of cloudy starter culture the next day signifies bacterial growth. The starter culture is scaled up for optimal bacterial cell growth by adding it in fractions into 2-3 liters volumetric flasks of TB media. This step is quickly followed by the re-addition of 1ml of 50mg/ml of kanamycin or ampicillin to each 1-liter flask containing TB media depending on the vector used. Allowing for peak logarithmic growth, the cell cultures are placed in a shaking incubator at 37°C for 2 hours 30 mins and/or until an absorbance range between 0.8 - 1.4 at 600 nm wavelength (OD600) is attained.

To induce optimal growth of the targeted heme protein in the bacterial cells, 0.22 g/l each of Isopropyl β-D-1-thiogalactopyranoside (IPTG) and Aminolevulinic acid (ALA) is added to the cell cultures after absorbance check. This was done by adding 0.48 g of ALA and 0.96 of IPTG to 2ml of distilled water. ALA is a precursor for the formation of the heme group and

IPTG helps to induce ample growth of the targeted protein. The reagent powder was mixed and vortexed into a solution. To initiate expression of desired heme protein, 1 ml of the resulting solution was aliquot to each 1-liter flask making up 3-liter cultures total. Lastly, the 2-liter cultures are subjected to decreased growth temperature of 32°C and then placed in the shaking incubator for 2-3 days.

2.5 Protein Harvest

CYP4X1 protein is harvested by collecting aggregated pellet of bacterial cells. This is achieved by aliquoting optimally grown *E. coli* JM 109 cells into centrifuge tubes to spin at 4200 rpm for 15 mins. Cell pellets showing requisite heme-thiolate reddish brown coloration are collected after centrifugation and solubilized in resuspension buffer while the supernatant is discarded by adding bleach. Cell pellets in resuspension buffer are stored at -80°C or immediately deployed for the next phase, which is cell lysis and membrane protein extraction.

2.6 Cell Lysis and Protein Extraction

Extraction of intracellular membrane proteins initially requires cell lysis which basically is the breaking apart of the phospholipid bilayer for accessibility. This process involves a combined use of sonication (a form of mechanical disruption) and application of detergents. To accomplish this for my project; frozen *E. coli* JM109 cells solubilized in resuspension buffer which contains the membrane heme protein CYP4X1 is thawed at room temperature water for about 20 mins. The thawed sample is sonicated on an ice bed 3 times for 30 seconds whilst waiting 30 seconds interval between each ultrasound exposure. Once the cells are lysed, Cymal-5 is added to the sample, then the cell pellets are stirred on an ice bed for 1 hour using a magnetic

stirrer. This helps to solubilize the proteins of interest, making it easier to extract hard to reach membrane protein. To calculate the amount of Cymal-5 added to enable protein extraction is as follows:

3.2 mM x ____ mL sample x 494.5 g/mol = _____/1000/1000 = _____ g Cymal-5.

The 3.2 mM of Cymal-5 is based on the critical micelle concentration, that is the lowest concentration where micelle formation will occur. 494.5g/mol is the molecular weight of Cymal-5. The subsequent divisions by a thousand (twice) is to adjust for S.I unit conversions from millimolar to molar and from milliliter to liter respectively.

2.7 Centrifugation

Utilizing centrifugal force to separate proteins based on their physical properties like solubility, size, shape, density is commonplace in bioanalytical chemistry. Centrifugation was first used to harvest cell pellets after 48 hours of scaled-up growth. Also, after solubilizing target membrane protein using Cymal-5 in the extraction phase. The resulting solution is cold centrifuged at 15000 rpm for 20 mins to isolate solubilized protein. Soluble liquid heme protein (lysate) is saved for purification via affinity and ion-exchange column chromatography while the cell pellet is discarded after adding bleach.

2.8 Protein Purification Protocol

Purification method used was low pressure liquid chromatography. Chromatography techniques separate mixtures based on interaction and speed at which the components move through special media contained in a matrix. In principle, low liquid pressure was used to move sample (protein) mixture through a packed stationary phase column affixed with specialized

material (Ni-NTA, Cobalt, CM and DEAE). The mobile phase solvent was set up with buffers indicated in the buffer table (Table 1) and liquid protein mixture; to be separated based on their characteristic interaction with the stationary phase material while eluting into a fraction collector using differential buffer environment and/or retention times.

Resuspension buffer and wash buffer used for this research had negligible interference with the sample to be separated because the pH (7.4) of the buffer is lower than the isoelectric point, pI (8.3) of the protein. The value difference has to be ensured or else, the surfaces of the protein will be largely negatively charged instead of neutral. Thus, repelling each other. Ensuring optimum pI is essential to the aggregation of protein in buffer solution.

Elution buffer on the other hand contains imidazole which helps to detach the binding of column matrix (cobalt or nickel) with the six-residue histidine tagged protein. Also, Cymal-5 was added to the buffers at some point in the research as a form of adaptation to methodology during experimental troubleshooting. Cymal-5 amphiphilic properties enables an interaction between its hydrophilic end and the hydrophobic membrane protein. Thus, keeping the protein soluble outside their core phospholipid bilayer.

2.8.1 Preparing column and mobile phase. The extraction lysate after centrifugation during was subjected to affinity column chromatography using cobalt or Ni-NTA (Nickel charged affinity resin). This was done by first setting up the stationary phase column with for example, 5ml of Ni-NTA beads contained in a slurry of buffer. The lysate is then added to the column. Then, the mobile phase is set up starting with resuspension buffer, followed by wash buffer and then elution buffer. Before purification begins, the slurry of buffer is allowed to flow through the column, then resuspension buffer is running through the aa beads into the fraction collector using a Bio-Rad biologic LP chromatography. The procedure for loading lysate,

rinsing, washing, and eluting the protein of interest was programmed alongside the allocation volume and the timeline prior to start of the purification protocol. Flow through is collected during the column purification process by a fraction collector.

2.8.2 Loading protein sample on beads. Soluble liquid CYP4X1 protein is suctioned onto the Ni-NTA (nickel beads) by the Bio-Rad Biologic LP chromatograph. The beads turn red as the heme-thiolate protein binds. This was made possible by the 6-residue histidine tag affixed to the protein during Protein expression.

A 100 ul fraction of the heme protein solution that flows through is collected into an Eppendorf tube and labelled ‘’Flow-through’’). 20 mL re-suspension buffer is added to the column.

2.8.3 Wash the beads. 20 ml of wash buffer is suctioned into the column and passed through the Ni-NTA beads. The wash buffer contains a low concentration of imidazole to remove weakly binding proteins.

2.8.4 Elute the protein. Protein is eluted from the column by adding 30 mL of elution buffer which contains high concentration of imidazole to remove all protein bound to the column.

2.9 SDS Poly Acrylamide Gel Electrophoresis (SDS-PAGE)

Sodium dodecyl sulfate polyacrylamide gel electrophoresis (SDS-PAGE) is used to separate proteins based on their molecular weight through a specialized gel matrix. SDS-PAGE helps to ascertain the presence and purity of the CYP4X1. The SDS part contains an anionic detergent carrying negative charges which is used to invalidate the intrinsic positive charges of the proteins thereby giving them equivalent charge and mobility in an electric field. Another reagent β-mercaptoethanol (BME), a thiol-reducing agent included in the sample preparation step

helps to denature the three-dimensional structure of the protein. The denatured protein(s) is/are attracted and move towards an applied electric field based on their mass-to-charge ratio. Thus, smaller proteins migrate faster through the gel matrix due to less resistance in moving through the porous layers. The presence of Cytochrome P450 protein (CYP4X1) is a horizontal band around 50kDa which is obtainable across the collected affinity chromatography fractions namely, flowthrough, rinse, wash, and elution.

To accomplish this, a Bio-Rad gel is obtained from refrigerated storage and used to set up the gel apparatus in the inner compartment of an electrophoretic box. The refrigerated gel and the gel dam are put together into a clamped frame or sealed gasket forming the inner compartment, the inner compartment is then secured in a casting gel-box stand. If properly done, the entire set-up should be leak-proof. Electrophoretic buffers are poured until they overflow on the inside chamber, as well as a marked buffer limit on the outside compartment. After the gel apparatus is fully assembled, a plastic comb atop the anionic gel is gently removed. The samples are added into the gel wells in a stepwise fashion using a micropipette with specialized tip; Firstly, a protein ladder containing pre-stained molecular weight marker is added to well number 1; this is followed by the chromatographic eluates in the order of flowthrough, rinse, wash, and elution. The protein ladder enables the estimation of the molecular weight region for a variety of protein standards.

2.9.1 SDS-PAGE buffer and solution recipes. Coomassie Staining Solution: To make a 100 ml Coomassie staining solution, 0.25g of Coomassie brilliant blue R250 is added to a Wheaton bottle, then 10 ml of glacial acetic acid is added to the mixture. Finally, 90ml of EtOH: H2O (1:1 v/v) is added and mixed well.

SDS-PAGE 10x Electrophoresis Buffer:

10x electrophoresis buffer comprises of: 25mM Tris, 192 mM glycine, 0.1% SDS, pH 8.3. To make this, 30 g of Tris base, 144 g of glycine, and 10 g of sodium dodecyl sulfate is dissolved in 950 ml of H_2O. The solution is made up to the 1000 ml mark. The pH of the buffer should be 8.3 with no adjustment required.

SDS-PAGE 1x Running Buffer:

Prepare 500 mL of 1x SDS-Page running buffer by adding 50 mL of 10X SDS-PAGE electrophoretic buffer to 450 mL of diH_2O.

2.9.2. SDS-PAGE sample preparation. Aliquot 10 ul of protein ladder into appropriately labelled Eppendorf tubes. Add 10 ul β-mercaptoethanol (BME) into ladder to achieve a final volume of 20 ul and concentration of 0.55M, mix well on shaker for uniformity. Repeat above protocol on the other eluates in the order of flowthrough, rinse, wash, and elution. Take note of the gel well numbers viz-a-viz sample descriptions, concentrations and loaded volumes.

2.9.3. SDS-PAGE protocol. Aliquot 10ul of sample mixture into gel wells starting with the protein ladder. Cover the chamber and firmly connect both the anode and the cathode. Set the voltage on the electrophoresis power supply to a constant voltage of 210 and turn on the instrument run. Allow the gel to electrophorese for 45–90 minutes or till the dye front gets to the bottom of the gel plate. Then the device power is turned off. Disconnect the electrodes and remove the cover. Remove gel holder from the electrophoresis chamber. Carefully remove the gel from holder. Remove the gel from its plates and proceed to staining with Coomassie blue. Coomassie blue staining and rinsing is done 3-4 times all whilst warming it up briefly in the microwave oven at intervals for 30 secs.

2.10 Protein Absolute Spectrum

Purified protein fraction eluted from Ni-NTA affinity low pressure liquid chromatography is subjected to UV-VIS spectrophotometry. Herein, Beer-Lambert's equation is applied to quantify the amount (concentration) of CYP4X1 based on the absorbance of the heme which is specific for CYP4X1. This is done by baselining and autozeroing the UV-VIS set at wavelength of 750nm – 250nm with Elution/Wash Buffer. Thereafter, 750mL of eluted protein fraction is placed in a cuvette at the wavelength range and ran for absorbance. The concentration of the obtained protein is then calculated by applying the Beer-Lambert's equation of $A = \epsilon Cl$. Where A = Absorbance

C = Concentration

ϵ = Molar Absorptivity Constant where 0.1 $\mu M^{-1}cm^{-1}$ is the heme coefficient

l = Path Length.

2.11 Carbon Monoxide Difference Assay

The carbon monoxide (CO) difference assay tests for the active functionality of protein using UV-VIS spectrophotometer. An elevated shift in spectra to the right to 450 nm in comparison to the absolute spectrum which has a heme peak at ~ 410 nm is indicative of an active CYP450 protein. To accomplish this, the UV-VIS wavelength scan is set to between 500 nm to 350 nm. Then, 750µL of CYP4X1 fraction is placed into a cuvette. Sodium dithionite is added to the fraction as a reducing agent. The cuvettes containing the fraction are placed in the UV-VIS. The instrument is autozeroed and baselined with the reduced fraction. Then, we bubble 50 carbon monoxide bubbles into it. Afterwards, we take and observe the spectra for an elevated

right shift. The amount of active protein can then be quantified by Beer-Lambert's equation as described above. The molar absorptivity constant for CO bound heme is 0.091 $\mu M^{-1}cm^{-1}$.

2.12 Ligand Binding Assay

Ligand binding assays conducted evaluates the affinity of substrates like arachidonic acid, anandamide, eicosapentaenoic acid, docosahexaenoic acid, ketoconazole, and inhibitors like PEITC with the protein binding site. This is the first line of evaluation to determine what type of compounds and their analogues binds favorably to the protein, which is a precursor to determining the characteristic nature of that active site and by extension the protein itself. This ultimately helps to elucidate the structure-function relationship of that protein.

To do this, 750µL of 1 µM protein fraction is added into 2 cuvettes: representing reference and sample. Both cuvettes are placed in UV-VIS and the wavelength scan is set from 500nm to 350nm. CYP4X1 protein (4.1uM) obtained from affinity column is converted to 1 mM using the formula: (750L) (1µM) = X µL (4.1µM). Then resuspension buffer amount used for dilution is 750 µL minus X µL Then the amount of stock (X) to add to sample cuvette is calculated by using the following formula: (0.5µM) (750µM) = (500µM stock) (X µL).

Same volume of ethanol is added to the reference cuvette. A 7-minute wait is observed before running each sample after the addition of varied and calculated amount of substrate (ligand) and reference (ethanol) to allow time for protein and ligand to bind.

This experiment is carried out until the observable peak and trough spectral shift in the UV-VIS spectra becomes uniform. The binding affinity data obtained is evaluated using Prism8 software.

CHAPTER 3 - RESULTS

This research involved attempts in elucidating the structure of CYP4X1 which is a finicky membrane protein. Data reported here are from optimized protein expression protocols for CYP4X1, narrative and pictorial representation of protein extraction and purification progress using several column chromatography techniques. We measured the absolute protein content and carbon monoxide difference assay via UV-VIS to show the concentration of active protein. We then used the purified protein for substrate binding assays and to screen for crystal hits. However, a significant portion of the results came from the optimization of expression protocols for CYP4X1 in *E. coli* JM 109 cells and the associated purification. Vectors used to accomplish cell transformation with CYP4X1 gene was alternated between two plasmids, pET28a and pCW.

3.1 Protein Expression and Purification

Preparing and autoclaving growth media and buffers like lysogenic broth, terrific broth as well as phosphate buffers preceded any inoculation for starter culture or Protein expression attempt. The first attempt on CYP4X1 Protein expression was with the pET28a vector purchased with the codon optimized CYP4X1 gene into JM109 cells in pre-prepared glycerol stock. The goal then was to translate it into proteins via induction with IPTG of *E. coli* JM109 cells. A starter culture was initiated. 10µl of the glycerol stock was pipetted into autoclaved 100 ml LB media, then 100 µl of antibiotic stock (50 mg/ml kanamycin) was added and the mixture was shaken overnight in an incubator at 180 rpm and 37°C. The starter culture shown in Figure 3 gave excellent turbidity demonstrating good bacterial growth.

Figure 3: Starter culture for CYP4X1.

25 ml each of the overnight starter culture was split equally between 2 liters of TB media for cell growth scale up. This was followed by the addition of 100 ml of potassium phosphate solution and 1 ml of 50 mg/ml kanamycin sulfate (antibiotic stock) solution to each 1-liter TB media. The cells were allowed a 2-hour timeline to grow, thereby allowing for an applicable phase of cell increase before it is induced for optimum protein yield using isopropyl β- d-1-thiogalactopyranoside (IPTG) and delta-aminolaevulinic acid (ALA). After a further two-day cell growth at 32 ℃, the protein expressing bacterial cells were harvested by centrifugation at 6000 rpm and showed an incorporated heme cofactor evident by a characteristic brick-red coloration.

After harvest, the pelleted cells were mixed in a resuspension buffer (1M Tris pH 8.0). To break the cells for access to the membrane protein, the resuspended pellet was sonicated on ice for 30 seconds at 80 percent with 30 second breaks three times. This was followed by membrane protein extraction via proprietary detergent (Cymal-5) which gave a reassuring brick red coloration. After stirring with detergent for 1-hour, solubilized protein was isolated by centrifuging at 20,000 rpm for 20 minutes. This was quickly followed by double chromatographic purifications via cobalt affinity and ion-exchange columns.

Figure 4 below shows harvested cell pellets, detergent extracted lysate, and banding on the gravity based cobalt column chromatography purification from the first attempt.

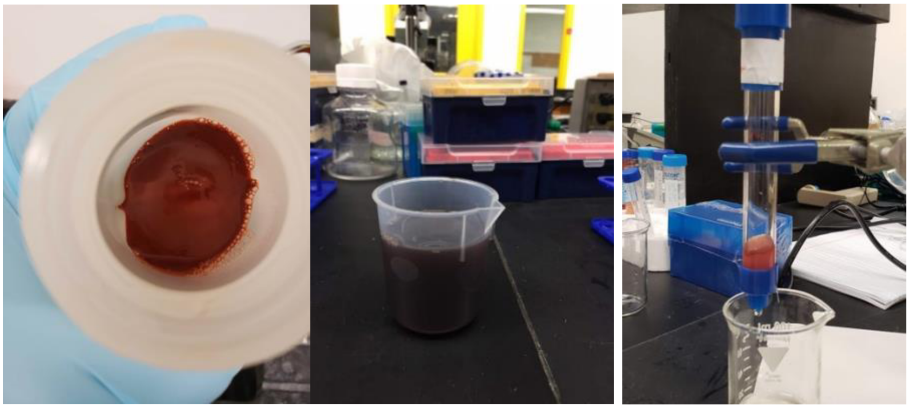

4: Pelleted *E.* coli cells, lysate after detergent extraction and lysate on cobalt column.

For this first attempt at Protein expression and purification via pET28a, the purified protein yield obtained after the ion exchange elution step was low as evident by the very small peak near 400 nm in Figure 5.

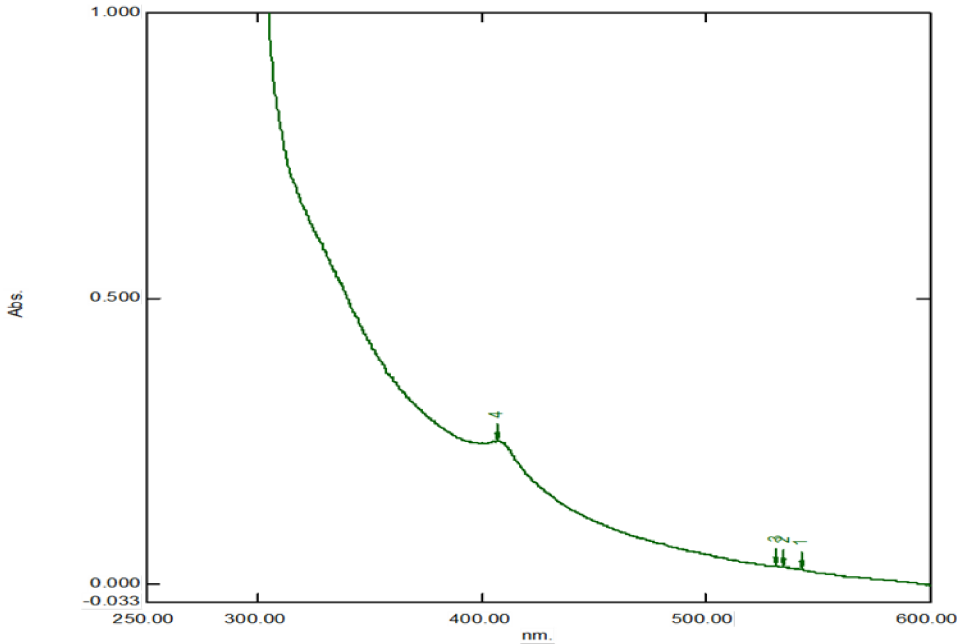

Figure 5: UV-VIS spectrum of purified pET28a CYP4X1 protein.

The CYP450 protein yield was not pure as the 280nm peaks is saturated. SDS-PAGE gel images illustrated in Figure 6 show lack of clean identifiable single bands at 50kDa despite applications of two gravity-based column chromatography purifications. This is possibly due to the presence of other macromolecules. Perhaps size exclusion column matrix would have significantly helped in the purification. Most of the applicable protein possibly came off the cobalt matrix in the wash phase or prior due to the deep red color obtained in the collected fractions.

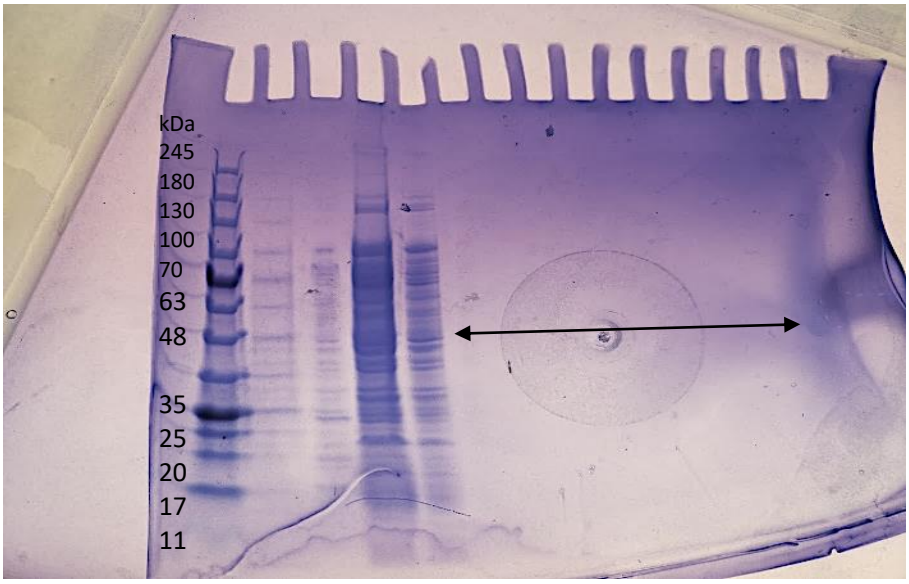

Figure 6: Electrophoretic gel of pET28a CYP4X1; Left-to right shows bands for protein ladder, flowthrough, rinse, wash phase and elution fractions from the cobalt affinity column.

3.1.1 A second protein expression. The experiment was repeated with modifications to the purification protocols. The lysate was run through serial column chromatography purifications; this time with a newly acquired Bio-Rad biologic LP autosampler and fraction collector. Also, the wash phase and elution from the cobalt (cobalt beads) affinity purification were combined prior to the start of ion-exchange purification. Eluates (wash and elution) from affinity column purifications was subjected to 10 times dilution with ion exchange wash buffer.

This was followed by the addition of 0.2057g Cymal-5 detergent; although, it should have been 0.2374g based on the volume of the combined cobalt column protein wash and elution fractions; there was not enough detergent at the time. Extraction detergent (Cymal-5) was added to the sample mixture to prevent crashing of target membrane proteins on ion-exchange column matrix and to aid with elution. Fractions of the ion exchange flowthrough and elution and cobalt rinse, wash and elution were collected and analyzed by SDS-PAGE. Upon investigation of stained gel using Coomassie blue, the SDS-PAGE purity check came out no identifiable CYP450 bands at 50kDa.

3.1.2 Change to pCW vector. A vector change was adopted for the third Protein expression attempt, A new glycerol stock carrying the CYP4X1 gene cloned into pCW. The antibiotic stock was also changed to ampicillin (50 mg/ml) from kanamycin sulfate because pCW carries the ampicillin resistance gene. Obtained cell pellets showed a coffee-brown coloration upon harvest at 6000 rpm, which was not expected as the previous brick red coloration was anticipated. As a result, it could be inferred that either the pCW vector did not properly translate the encode gene for the heme-thiolate prosthetic group or the polynucleotide sequence is erroneously put together during gene construct.

3.1.3 The third protein expression and purification. Experimental trial was executed to the end with membrane protein extraction and cobalt affinity column purification only. Purification results obtained showed that most of the proteins eluted at the wash stage and practically no protein was obtained from the elution. This was ascertained upon protein absolute spectra analysis. SDS-PAGE analysis of collected affinity column fractions came out negative for the target protein (CYP450). No ion-exchange purification was conducted. It was surmised that perhaps the cells were not within the right optical density range before induction.

The cells were initially allotted a 2-hour time lapse at 37℃ to accommodate for the appropriate stage of growth without intermittently checking for an optimal OD_{600} absorption value range of 0.4 -1.2.

3.1.4 The fourth protein expression and purification. Executed protocol adjusted for a OD_{600} > 0.4 for the grown cells as recommended in related literature (Stark, Dostalek and Guengerich, 2008). Also, a fresh colony was selected after DNA transformation instead of a glycerol stock approach.

For the DNA transformation, *E. coli* JM109 cells in Eppendorf tubes were thawed on ice. 1 µL pCW vector carrying the target gene was aliquoted into the cells. The resulting mixture was left on ice for 30 mins then placed in warm water at 37℃ for 35 seconds to heat shock cells. The mixture was returned on ice for 2 minutes; giving the cells a chance to recover. 50µL of the transformed cells were place at the center of LB-agar culture plates; glass beads were added to spread the cells across the agar containing plates before being safely discarded. The plates were incubated overnight at 37℃.

Using a pipette tip, a single colony of transformed cells was selected and emptied into 100ml of autoclaved LB media before incubating overnight at 37℃ and 180 rpm. The sample which is the starter culture showed excellent turbidity. The rest of the experimental attempt followed previous Protein expression protocols. The OD_{600} was at 0.44 before induction. Still, the harvested cell pellets gave a coffee-brown coloration as shown in Figure 7.

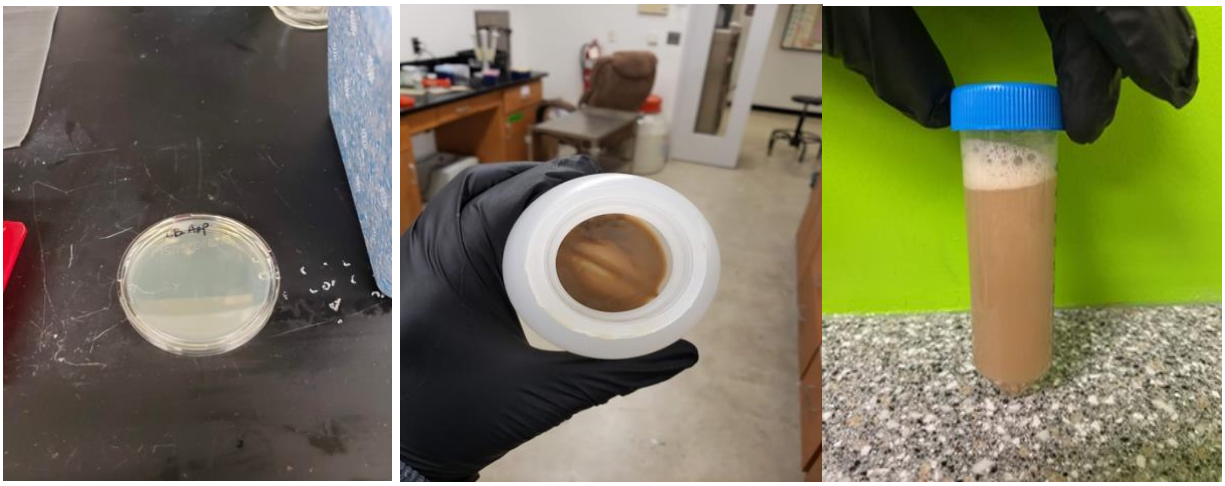

Figure 7: Images from pCW4X1 protein expression process. From left to right, culture plates after transformation via heat shock, JM109 cell pellets showing coffee brown color instead of brick red after harvest via centrifugation, pelleted cells homogenized in resuspension buffer.

Interestingly, the anticipated heme-thiolate color improved slightly upon detergent extraction on ice as shown in Figure 8. This corroborates the impact of Cymal-5 on membrane protein extraction.

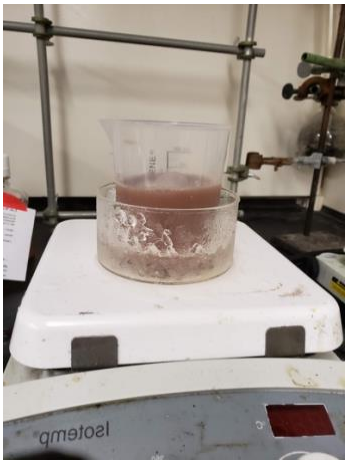

Figure 8: Detergent extraction via cymal-5 for pCW4X1

This purification followed the same basic protocol as the first purification, the lysate after centrifugation was purified by affinity and ion-exchange purification protocols with fractions collected. Afterwards, a UV-VIS spectrophotometric analysis of elution ensued for absolute

protein and carbon monoxide difference assay. A peak at around 400nm, which is customary to CYP450 was obtained for the protein's absolute spectrum. This validates the presence of heme in the lysate solution containing CYP 4X1.

Typically, proteins carrying a heme cofactor have peaks around 400 nm while proteins carrying amino acids like tryptophan, tyrosine and phenylalanine in their sequence give peaks around 280nm. CYP4X1 being a characteristic cytochrome P450 meet both criteria.
Thus, from the spectra below, closer to 1:1 ratio of 400 nm peak to 280 nm peak indicates increased purity of CYP4X1 protein. (Ortiz de Montellano, 2015).

The pCW CYP 4X1 protein was much purer due to the additional ion exchange purification step using Bio-Rad biologic LP autosampler and fraction collector. Figure 9 below illustrates this. When compared to gravity, the application of low solvent pressure via the autosampler and fraction collector increases accuracy, integrity and overall resolution of chromatogram peaks due to better interaction between the solubilized protein and the stationary phase matrix.

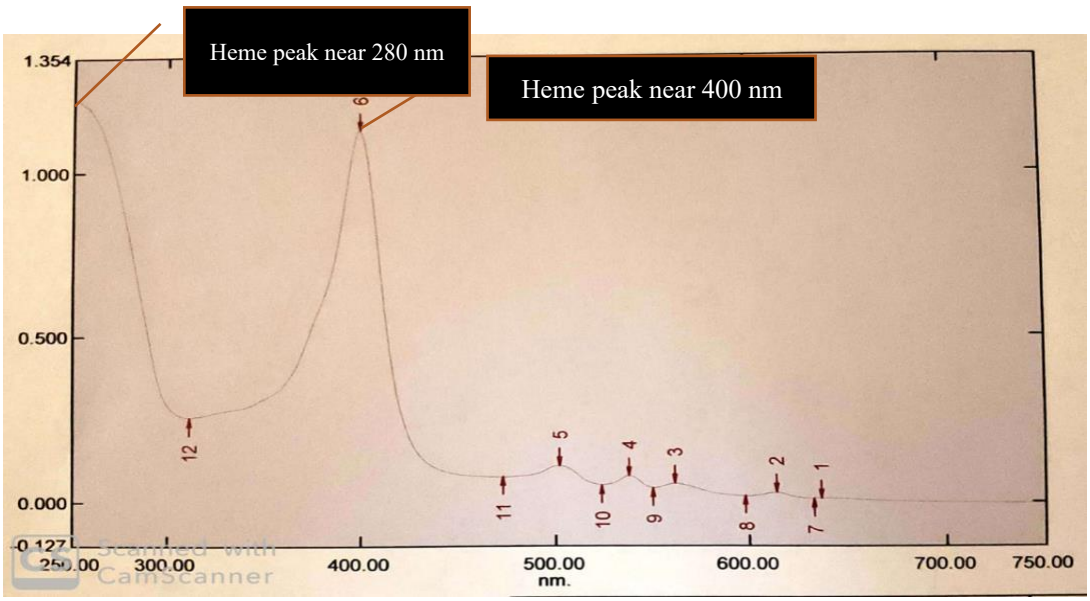

Figure 9: UV-VIS spectrum of purified pCW CYP4X1 following ion exchange.

After the absolute protein spectra analysis, a quick carbon monoxide difference assay is conducted wherein CO gas is bubbled into the lysate upon the addition of sodium dithionite (a reducing agent). Spectra shift to the right indicates the presence of active CYP 450 proteins, which was exactly the case in Figure 10.

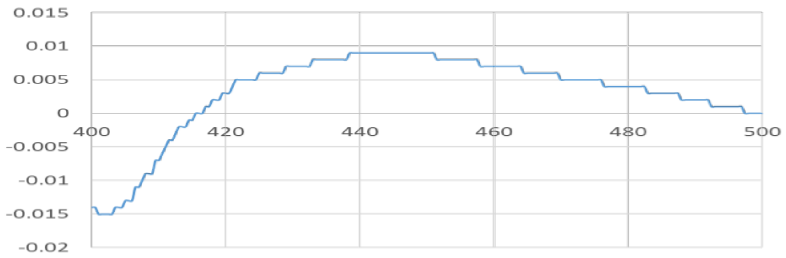

Figure 10: Binding of carbon monoxide to reduced pCW CYP4X1.

The SDS-PAGE analysis of the chromatographic eluates from both affinity and ion exchange column yielded a positive data but faded banding at 50kDa region as evident in the stained gel images in Figure 11.

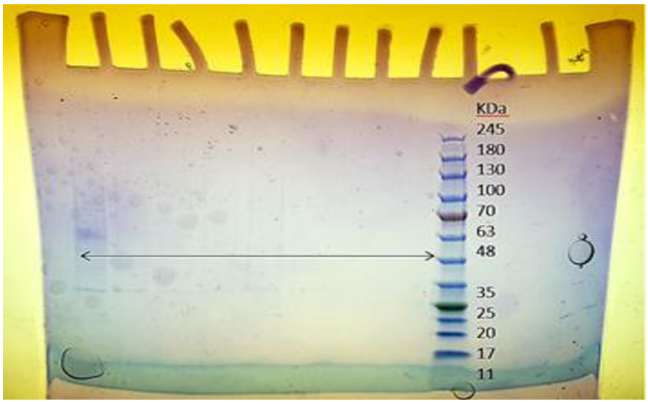

Figure 11: Electrophoretic gel of pCW4X1 with bands near 50 kDa. Right to left shows bands for protein ladder, flowthrough, rinse, wash phase and elution fractions from the cobalt affinity column, plus ion-exchange wash and elution.

3.1.5 The fifth protein expression. Experimental attempt was initiated but this time doubling the volume *E. coli* cells inoculated. The cells pellets obtained after harvest was still coffee-brown in coloration and the general results largely the same. The concentration of the obtained protein was too low for characterization.

3.1.6 Return to pET28a plasmid. As a result of purification successes with the pCW vector derived protein, but with very low yields, a decision was made to return to the pET28a vector which seemed like it had better expression levels of CYP4X1.

3.1.7 The sixth protein expression. Experimental attempt involved a return to pET28a plasmid carrying CYP4X1 into JM109 *E. Coli* cells in a glycerol stock. Ample OD_{600} range of 0.4- 0.8 prior to induction was also maintained. The expression protocol yielded cell pellets with characteristic brick red (reddish brown) coloration upon harvest. This purification attempt of these cells included experimental tweaks to optimize for obtaining the quantity and quality of the membrane protein. The protocol change began with lysate acquisition via centrifugation following sonication of cell pellets and detergent extraction of membrane proteins. The cold centrifuge was increased from 15,000 rpm for 20 mins to 19,000 rpm for 20 mins. Increase in rpm yielded a thick, slimy, deep red lysate previously unattained.

The lysate in this experimental attempt had much better overall consistency and richness compared to those from previous protocol. Affinity chromatographic column via Bio-Rad LP autosampler and fraction collected was initiated using nickel beads instead of cobalt. This switch was made following an observation of another graduate student with a different protein that their protein bound to a nickel affinity column but not a cobalt affinity column, which was previously

used because His-tagged proteins have been reported to be purified with higher purity with cobalt beads.

Just like in the lysate as explained in the methods chapter, Cymal-5 detergents were also added to affinity column purification buffers in the following details:

- Buffer A (Resuspension buffer) - 60 ml x 3.2mM X 494.5g/mol = 94944 / 1000ml /1000 = 0.095g of Cymal-5 added.
- Buffer B (Wash buffer) - 40 ml x 3.2mM X 494.5g/mol = 63296 /1000ml /1000 = 0.063g of Cymal-5 added.
- Buffer C (Elution buffer) - 30 ml x 3.2mM X 494.5g/mol = 47472 /1000ml /1000 = 0.047g of Cymal-5 added.

CYP4X1 did not make it to the wash phase as protein was not binding to the nickel beads enough to create retention. Targeted protein was simply rinsed out of column upon the addition of resuspension buffer. Absolute protein spectra of column rinse showed an absorbance peak at 406 nm which is around 400nm with no corresponding (parallel) peak around 300nm.
This demonstrates lack of purity The protein concentration calculated using Beer-Lambert's equation to obtain a decent 22.8 mM. Carbon monoxide difference assay did not indicate the presence of active protein. SDS-PAGE-stained gel gave unusable bands across the purification eluates.

3.1.8 The seventh attempt on protein expression. pET28a was used with a core focus on optimizing nickel affinity purification. Although, this time the harvest for cell pellets was centrifuged twice at 5000 rpm. Also, centrifugation of detergent extracted protein was set at 19000 rpm for 20 min to obtain cleaner lysate. Lysate was subjected to nickel-based affinity column chromatography. Initial results show significant target protein coming off the wash

phase. This assertion was made via the graphical retention time (volume vs time) data obtained from the chromatogram. Lysate appeared to have crashed on the nickel column as it did not elute after the application of imidazole-based buffer. Using a slower gravity method, Buffer with increased concentration of imidazole (0.16g) was added to the nickel column to aid in the elution of the bound lysate. No protein eluted whilst using the increased imidazole elution buffer with the gravity technique; thus, confirming the crashing of the solubilized protein on the stationary phase matrix.

Ion exchange chromatography was carried out on the nickel affinity wash eluate. Fractions of nickel affinity wash eluates in tubes 38-42 (20 ml in total) were diluted with 80 ml of ion-exchange wash buffer containing Cymal-5. The resulting solution ran through the resins in the column matrix (CM) shown in Figure 12. Addition of the detergent to the ion exchange buffers were as follows:

- 80 ml x 3.2mM X 494.5g/mol = 126592 /1000ml /1000 = 0.127g of Cymal-5 added.
- 35 ml x 3.2mM X 494.5g/mol = 55384 /1000ml /1000 = 0.055g of Cymal-5 added.
- 55 ml x 3.2mM X 494.5g/mol = 63296 /1000ml /1000 = 0.087g of Cymal-5 added.

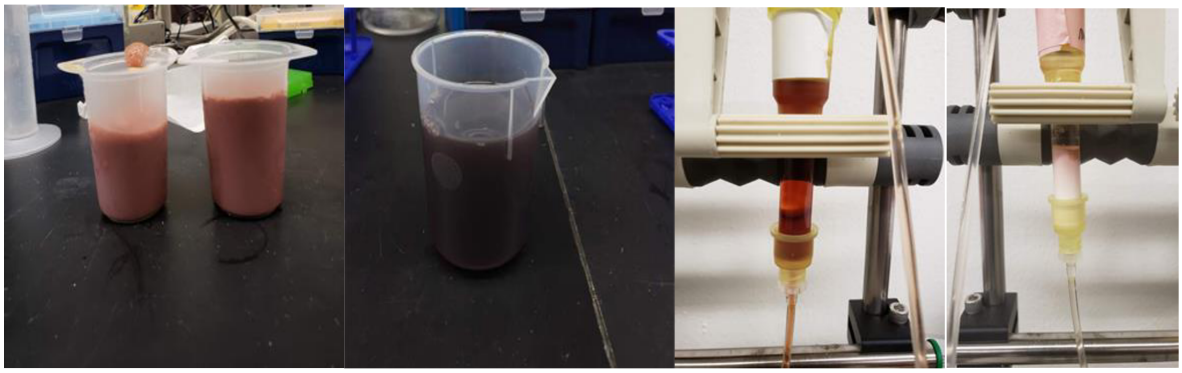

Figure 12: Images from the purification process. from left to right, lysed pelleted cells homogenized in resuspension buffer, centrifuged lysate decanted after detergent extraction, banding present on the Ni-NTA affinity column after loading protein, banding present on the CM column after loading protein.

I carried out absolute protein assay, carbon monoxide difference assay and SDS-PAGE on both nickel affinity and ion-exchange eluates. UV-VIS's data obtained for protein absolute spectra showed an absorbance peak of 2.554 around 400nm. Obtained protein concentration using Beer-Lambert's equation yielded a value of 25.54 µM which is good. However, the protein lacks optimum purity evident by the lack of a peak around 280nm in Figure 13.

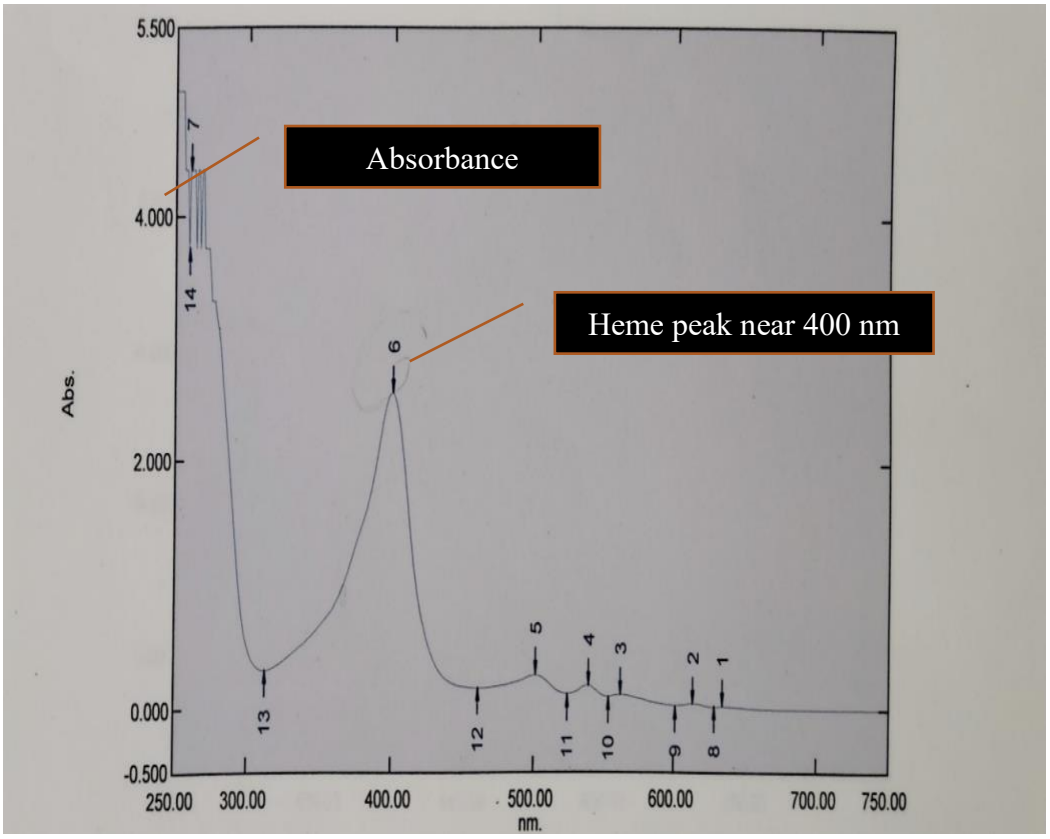

Figure 13: Absolute protein spectrum from the seventh purification protocol.

I tested for the presence of active protein after bubbling carbon monoxide into Ni-NTA column wash eluate and observed the characteristic right shift towards 450nm in Figure 14. Absorbance value was 0.142 and a corresponding concentration value of 1.56 µM which is considerably less than the total amount of protein present.

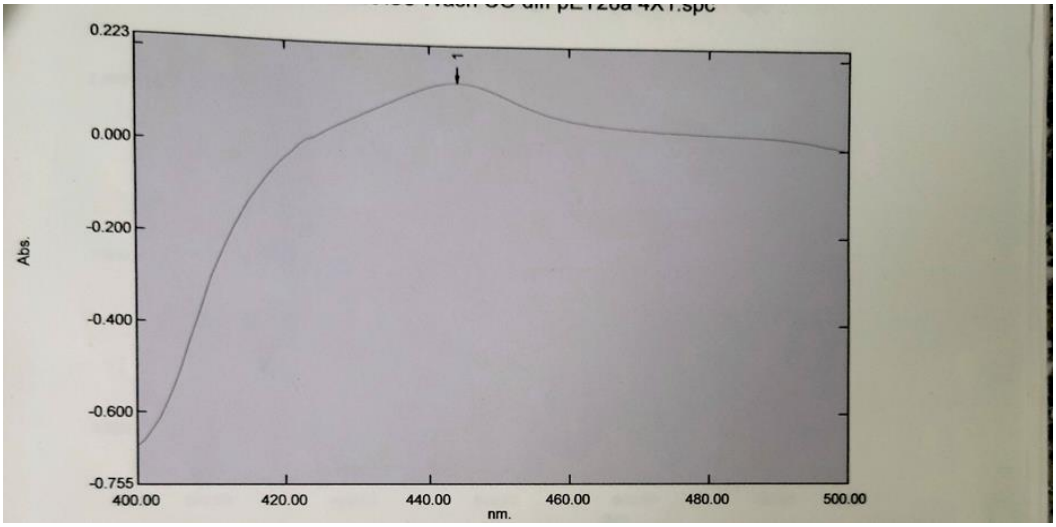

Figure 14: Carbon monoxide difference spectrum from the seventh purification.

Absolute protein spectrum from Figure 15 below illustrates lack of pure protein after carboxymethyl column purification.

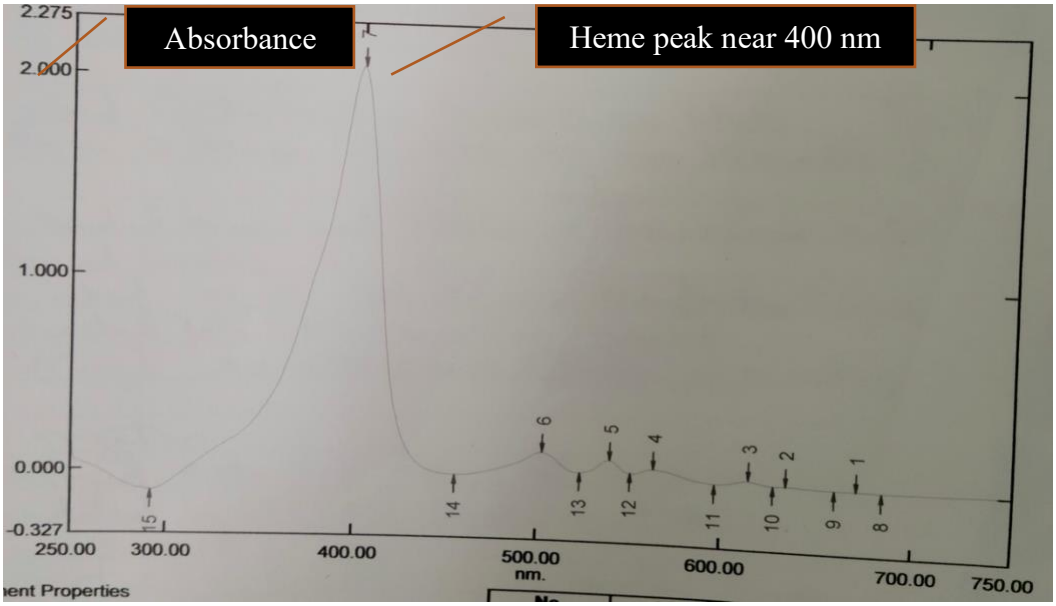

Figure 15: Absolute protein spectrum from CM column.

Carbon monoxide difference spectrum in Figure 16 shows the presence of active protein but low concentration after carboxymethyl column purification.

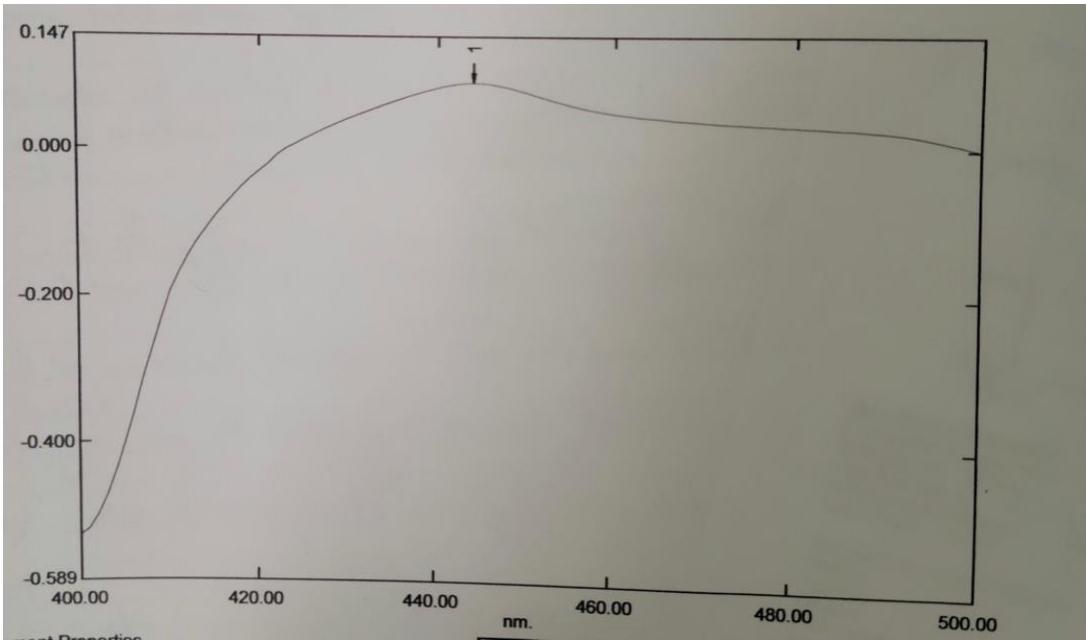

Figure 16 Carbon monoxide difference spectrum from CM column.

SDS-PAGE gel in Figure 17 below was badly stained and practically unusable.

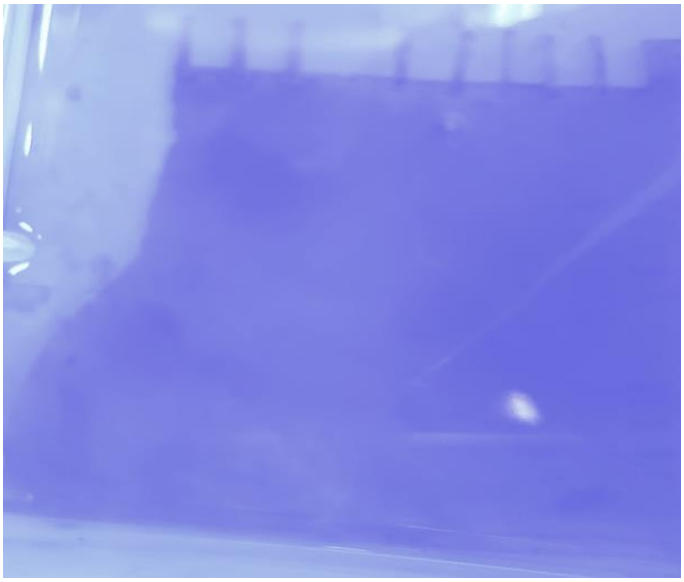
Figure 17: Electrophoretic gel from the seventh purification protocol.

3.1.9 The eighth protein expression and purification. Experimental attempt at characterization involved an increase in prepared growth media (terrific broth) used; from 2 liters

to 3 Liters. The idea was to significantly increase the amount of obtainable transformed *E. Coli* cells upon harvest. Experimental protocol was deployed smoothly until protein purification. Instead of tris buffers which were used on all purifications before this one, phosphate-based buffers were used. Unlike Tris, phosphate buffer mimics cellular pH environment near 7.4 better without adverse effects to cellular processes. Protein loaded well with lysate forming a decent ring around the Ni-NTA column evident in Figure 18. Data obtained from collected fractions showed that most of the target protein came off in the wash phase. Perhaps, the six residue his-tag was not properly transcribed during protein expression. 1ml of the Ni-NTA column fractions was preserved for gel electrophoresis. Tubes 63 to Tubes 75 representing 40 ml of wash phase fraction from nickel affinity column was diluted up to 160 ml with 120 ml of ion-exchange wash buffer. Cymal-5 was added to the diluted wash solutions for ion exchange column purification.

Figure 18: Pictures from the purification process. From left to right, pelleted cells after centrifugation, lysed pelleted cells homogenized in resuspension buffer, centrifuged lysate decanted after detergent extraction, banding present on the Ni-NTA affinity column after loading protein.

I carried out absolute protein assay on Ni-NTA column eluates. Absorbance value obtained is 0.612 as shown in Figure 19 and a corresponding concentration of 6.12 µM was obtained.

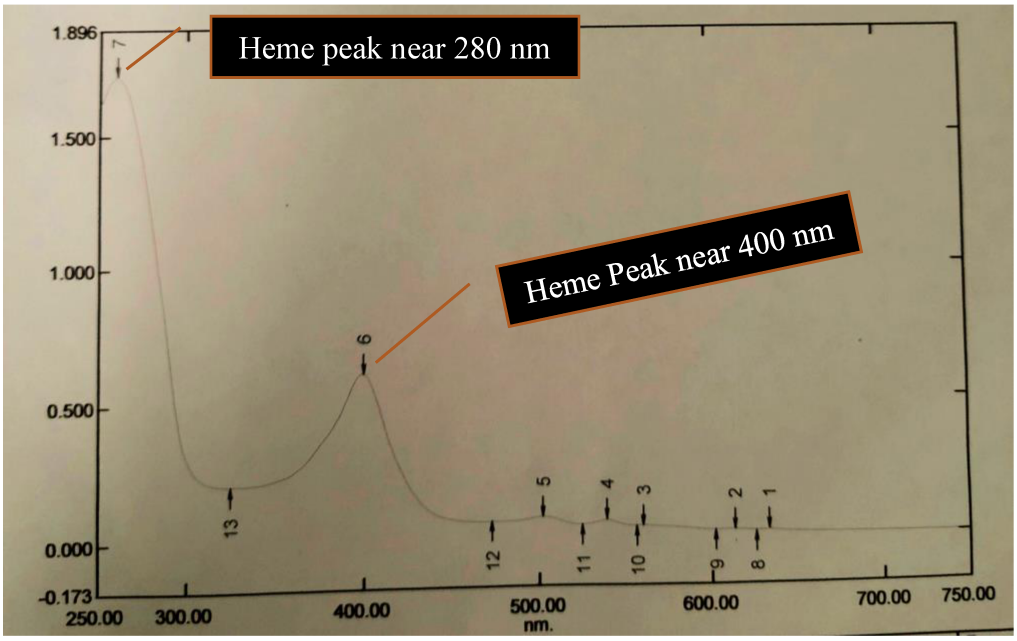

Figure 19: Absolute protein spectra of Ni-NTA column wash eluate.

I ran SDS-PAGE on protein ladder, Ni-NTA affinity (flowthrough, rinse, wash, and elution) and ion exchange (wash and elution) eluates. Gel disintegrated during staining and rinsing but the gel wells were still visible in Figure 20. Bands barely show any protein of interest.

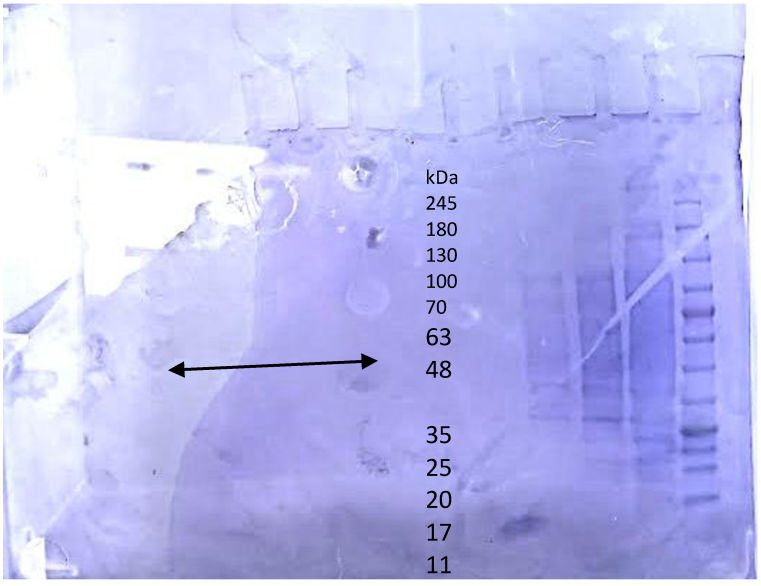

Figure 20: Electrophoretic gel from purification protocol. Right to left shows bands for protein ladder, flowthrough, rinse, wash phase and elution fractions from the Ni-NTA affinity column.

3.1.10 The ninth protein expression and purification. Experimental attempt followed previous working protocols but used Triton X-100 and CHAPS detergent (3-((3-cholamidopropyl) dimethylammonium)-1-propanesulfonate) as detergents for membrane protein extraction. This zwitterionic detergent(s) proves useful for membrane protein solubilization when it is important to maintain protein activity.

The extracted protein gave the best visible lysate obtained in the project thus far, judging by the unprecedented brick-red coloration, thickness, and consistency. One-third of this resuspended pellet (45ml) was subjected to chromatographic purifications while two-thirds were kept for later purification. With a return to Tris base instead of phosphate for the purification buffers; Triton X-100 and CHAPS were also included in the resuspension, wash and elution buffers used in purification buffers instead of Cymal-5 as follows:

CHAPS = 0.5% = 1 x CMCL = 0.5g / 100 ml = w/v

Triton x -100 = 1 x 0.04 = 0.9 ml/ 45 ml = v/v

For example, 60 ml of resuspension buffer with phosphate:

0.25/100 ml x 60 ml = 0.15 g of chap's detergent in 60 ml

(60ml) (0.04%) = 240 ml of Triton X-100 / 0.24 ml

Forty milliliters of wash buffer and 30 ml of elution buffer were also prepared using the same calculation for detergent addition to resuspension buffer. For Ni-NTA column purification, the lysate did not bind well to the nickel column despite giving the visibly consistent heme-based reddish brown colored lysate which probably had something to do with the detergent (triton and CHAPS) used for extraction and in the purification.

UV-VIS spectra analysis on absolute protein was best in the rinse giving peaks with an absorbance value of 0.612 near 400nm as evident in Figure 21. The protein concentration was

low with concentrations of 6.12µM. The affinity column rinse still showed the presence of active proteins with a right shift towards 450nm when carbon monoxide was bubbled through it. Ion exchange purification was not conducted as the purification was ended after Ni-NTA column.

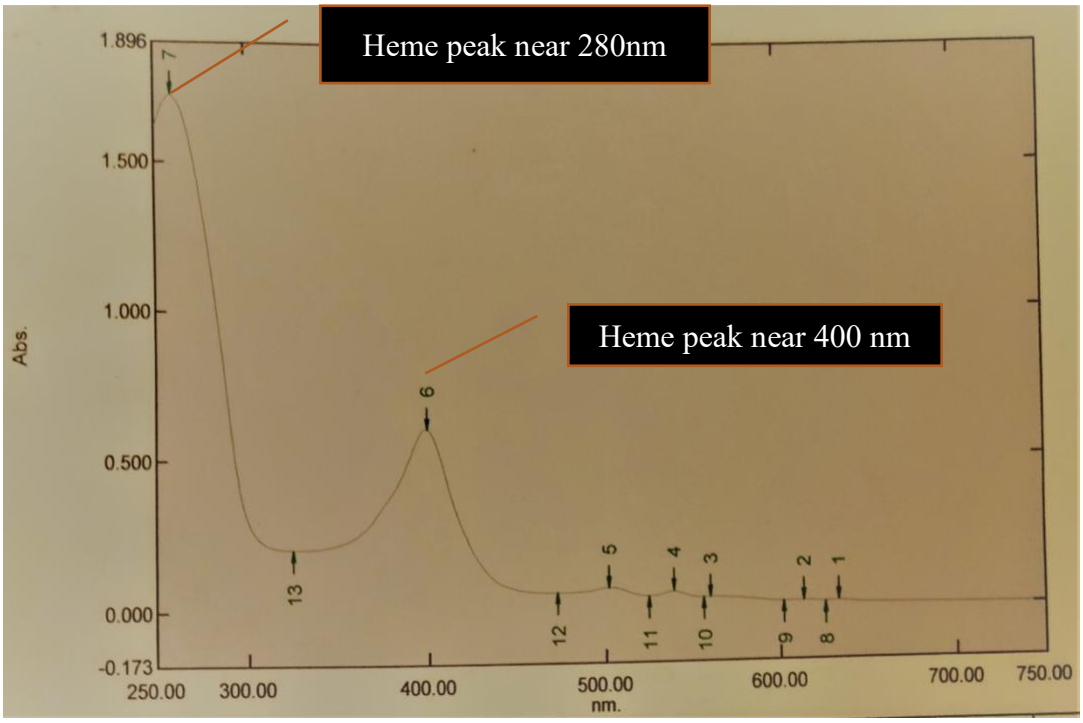

Figure 21: Absolute protein spectrum of Ni-NTA affinity rinse.

3.1.11 The tenth protein expression and purification. This experimental attempt used Cymal-5 and CHAPS as detergents for membrane protein extraction while Triton X-100 was discontinued. Every other pre purification parameter was maintained. Left over cell pellets from the ninth purification which makes up two-thirds of the former harvest was subjected to lysis via sonication on ice. This was followed by protein extraction was carried out on an ice bath for 1-hour using Cymal-5 and CHAPS.

CHAPS = 0.5% = 1 X CMCL = 0.5g / 100 ml = w/v

Cymal-5 = (100ml x 3.2 x 494.5) / 1000 x 1000 = 0.158g / 100 ml = w/v

The extracted protein was centrifuged at 19000 rpm for 20 mins. Cymal-5 was added to the Ni-NTA column buffers. The tenth protein expression attempt gave much better affinity column result than the ninth. However, the protein precipitated on the Ni-NTA column during the wash phase. Wash and elution buffers were combined; 0.66g more imidazole was added to the mixture to aid in the elution of the protein that precipitated on the Ni-NTA column.

45 ml of the wash phase eluate was diluted with 90ml of wash buffer. This is to adjust for concentration of salt content present. Cymal-5 was also included. The ion exchange purification results carried out were not great. Protein absolute spectra assay was conducted but results obtained were not usable either.

3.1.12 The eleventh protein expression and purification. Experimental attempt saw the application of a new gene construct of pCW 4X1. This was done to ameliorate the crashing of protein on the affinity resin, improve on low protein yield while anticipating an increase in the expression of the heme thiolate prosthetic group. A single colony from culture plates was inoculated into LB media. Thirty-three milliliters each of the cloudy overnight starter culture was aliquot into 3 liters of TB media.

1 ml of 50 mg/ml antibiotic (ampicillin sodium) stock was added and allowed to grow at 37°C with 180 rpm shaking. OD_{600} was at 0.5 after 3.5 hours. Induction using IPTG and ALA was initiated, and the culture was allowed to grow at 32°C, 180rm for 3 days. The obtained pellets upon harvest were still coffee-brown coloration. Protein extraction used Cymal-5 and CHAPS again just like it in the ninth expression attempt. For eluates obtained from Ni-NTA affinity purification, tubes 27-29 from the fraction collector was the elution with a light-yellow coloration. Absolute protein spectra in Figure 22 were positive but very low and impure for the

CYP 450 protein present. With an absorbance of 0.167 and a corresponding concentration of 1.67µM.

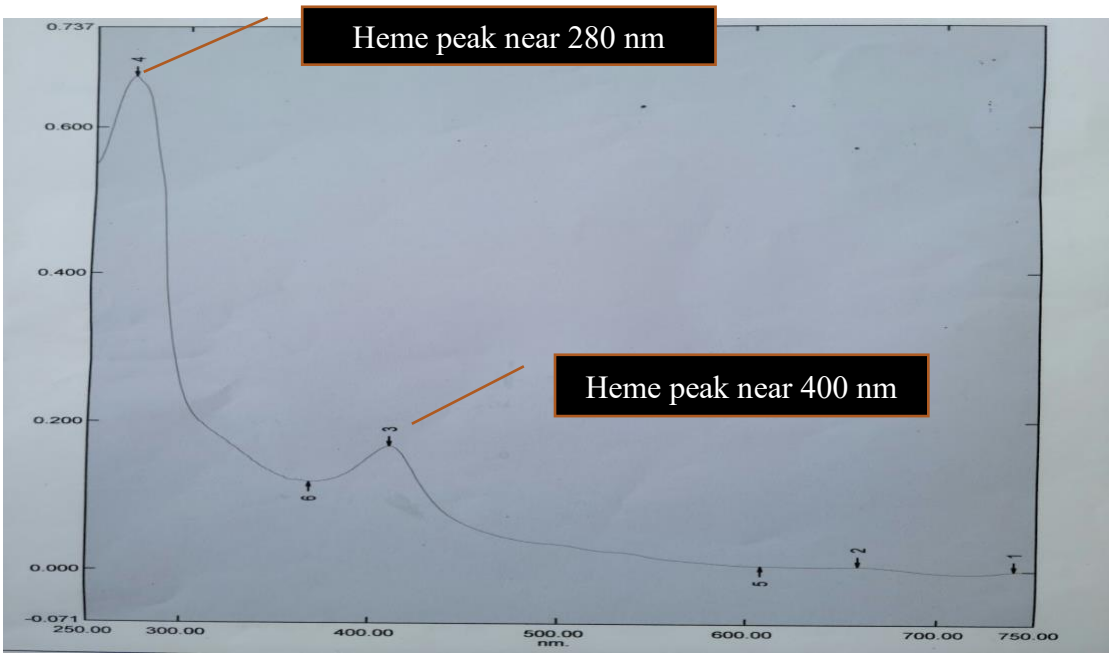

Figure 22: Absolute protein spectrum of Ni-NTA elution for pCW4X1.

The carbon monoxide difference assay was carried out for test protein activity, but the UV-VIS spectrum is not included here because concentration was nonexistent. Eluates from Ni-NTA was repurified on second column (DEAE). Ni-NTA column elution representing 12 ml was diluted 5 times to 60ml with 48ml ion exchange wash buffer and 0.076 g of Cymal-5. 50 ml of ion-exchange wash buffer was made with 0.079g of Cymal-5 also, 30ml of ion-exchange elution buffer was made with 0.047g of Cymal-5 added. For purification of Ni-NTA column purified protein elution, ion exchange worked better with DEAE than CM beads. Absolute spectra of elution from ion exchange purification were good. However, the concentration of the protein upon carbon monoxide was too small. 15ml of the elution from ion exchange (DEAE Column) was concentrated by spinning at 5000 rpm for 15 minutes. 2mL of concentrated protein was

added to 750 µL of ion exchange elution buffer present in UV-VIS cuvette. Remeasuring the absolute protein spectra in Figure 23 yielded an absorbance of 0.021 and a corresponding concentration of 0.21µM at wavelength of 406nm. Obtained lysate was reconcentrated further via a micro concentrator to 160µM with carbon monoxide difference assay shown in Figure 24.

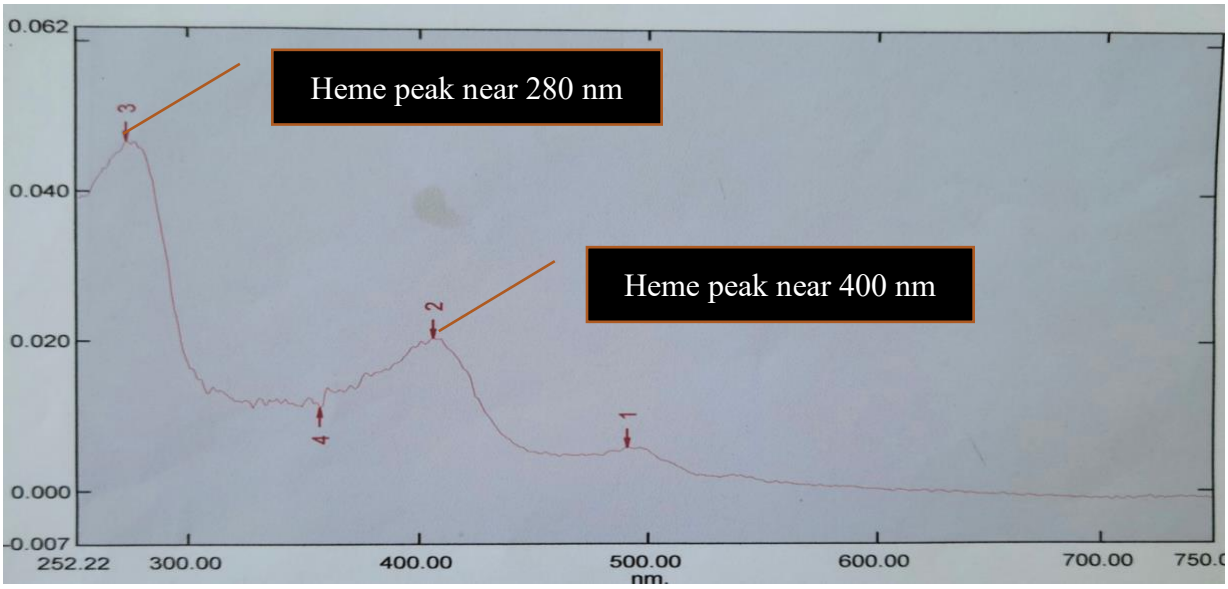

Figure 23: Absolute protein spectrum of re-concentrated DEAE ion-exchange elution.

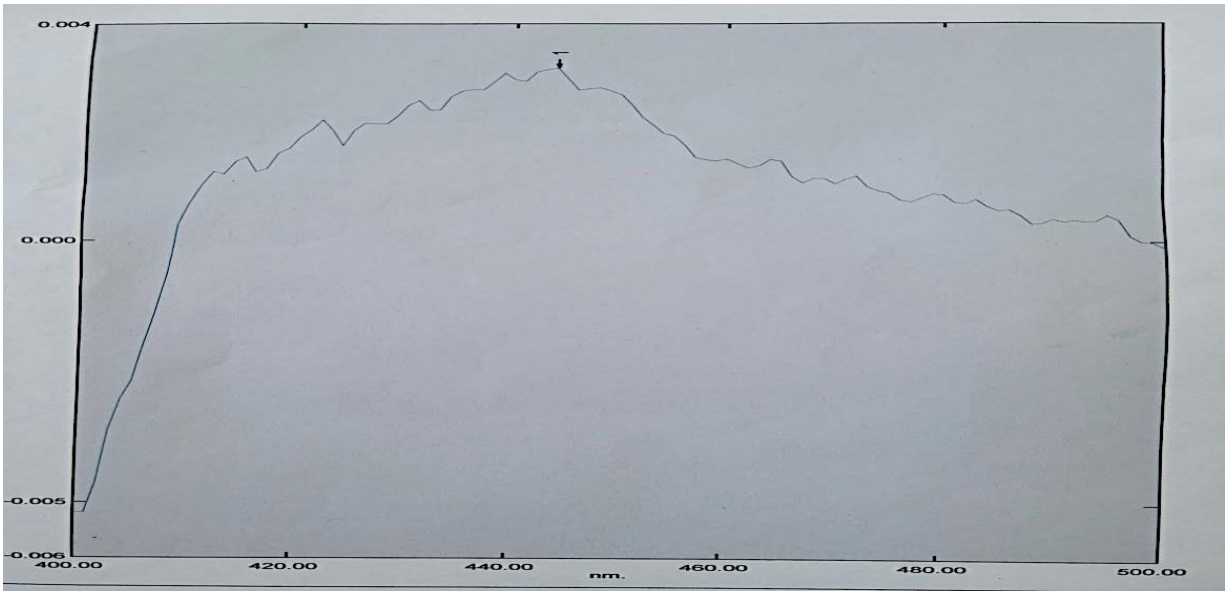

Figure 24: Carbon monoxide difference assay of reconcentrated DEAE elution.

I initiated SDS-PAGE of column eluates as shown in Figure 25. Affinity and ion exchange eluates showed excellent promise as the characteristic CYP450 band was clearly seen in the SDS-PAGE gel.

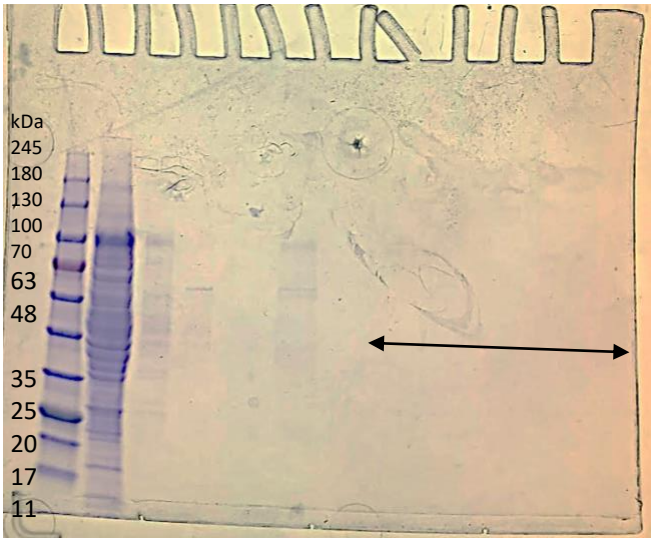

Figure 25: Electrophoretic gel showing bands for pCW4X1. Gel wells for eluates were as follows: Ladder, Ni-NTA flowthrough, Ni-NTA affinity wash, Ni-NTA affinity elution. Ion-exchange flowthrough, ion-exchange elution.

3.1.13 The twelfth protein expression and purification. Protocol involved a return to pET28a vector and kanamycin antibiotic stock. 20µl of glycerol stock was inoculated into 200ml LB media. The resulting starter culture was aliquot into 3 liters of TB media prepared for scale-up growth. The marked increase was done to significantly increase the amount of obtainable cell growth and by extension CYP450 protein. OD_{600} was at 0.72 prior to induction. 0.127g Cymal-5 and 0.393 CHAPS was used for protein extraction and stirred on ice for 1 hour. Extracted protein was centrifuged at 19000 rpm for 20 mins to obtain lysate. I subjected lysate to Ni-NTA column purification using nickel beads.

The absolute spectrum yielded characteristic CYP450 peak, but carbon monoxide difference assay gave low active protein. Despite this, the eluate was further purified by DEAE ion exchange for crystal screening setups. Elution and wash eluates were combined to make a total volume of 22 ml. These combined eluates were diluted five times by adding 88 ml of ion exchange wash buffer to make up 110ml. Cymal-5 (0.174g) was added to the mixture. Cymal-5 was also added to the ion exchange wash and elution buffer.

Post DEAE column purification, tubes 7-9 were put aside as flowthrough whilst tubes 27-29 were earmarked as elution. Protein assay to get absolute concentration from the second column elution was good as evident in Figure 26. Carbon monoxide difference assay for active protein after DEAE purification was still too low but more refined and purer. After carbon monoxide difference assay, the protein was concentrated in attempts to get a concentration of at least 1 µM for binding assays. Unfortunately, the volume of the multiple protein concentration efforts was not adequate for binding affinity but just enough for crystal screening. Attempt at commercial screening yielded crystal hits.

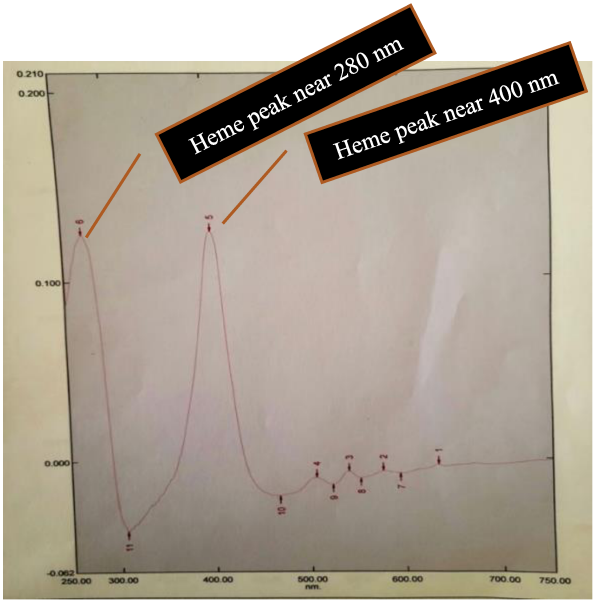

Figure 26: Absolute protein spectra from DEAE column (second) purification. Spectrum showing 1:1 soret peak ratio near 400 nm and 280 nm region.

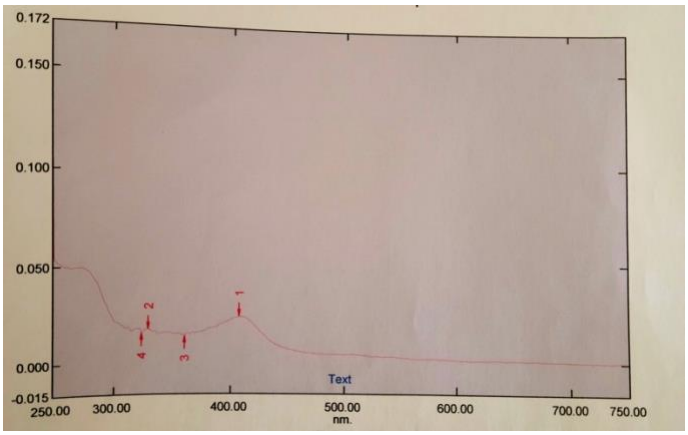

Figure 27: Absolute protein spectra from reconcentrated DEAE column (second) purification. Concentration obtained was approximately 0.24µM.

3.1.14. The thirteenth protein expression and purification. In this experimental attempt, CYP4X1 pET28a glycerol stock (10µl) was inoculated into autoclaved 100ml LB media. Added 100 µl of antibiotic (kanamycin 50 mg/ml sulfate). Shook overnight at 37˚C at 180 rpm in the incubator. I initiated growth scale up by adding 33ml of starter culture to each 1-liter TB media making 3 liter in total and added kanamycin antibiotic stock and optimize growth till OD_{600} of 1.24. To make inducing agent, 1.44g ALA with 0.72 g IPTG were all in 3ml distilled H_2O and one milliliter was distributed to each flask and left to grow for 3 days. Cultured cells were poured into eight 400ml containers and centrifuged at 4200 rpm for 15 mins. Bacteria pellets exhibited very brick red coloration.

E. coli pellets in resuspension buffer were lysed with sonication and subjected to Cymal-5 protein extraction and stirred on ice for 1hour. Extracted protein was centrifuged at 19000 rpm for 20 min. The lysate was retained, and I discarded the pellets. The lysate was subjected to Ni-NTA column chromatography.

The results showed protein precipitation on the nickel column with most of the CYP 4X1 protein eluting in the wash phase. The assertion was made based off retention peak vs time on the Bio-Rad fraction monitor. The CM column representing the second purification column on

wash eluates that came of the affinity column. Wash eluates were from tubes 19-22 for the nickel affinity column representing about 30ml. Wash eluate was diluted 5 times with 120ml of wash buffer and 0.1898 of Cymal-5 detergent. 35ml of ion-exchange elution and 55ml of wash was also furnished with Cymal-5 based on established calculation. Eluates from the purification were concentrated and tested for absolute protein spectra, carbon monoxide difference assay, crystallography and SDS-PAGE analysis.

For absolute spectra at 400 nm, an absorbance of 2.145 was obtained and this yielded a concentration of 21.45 µM. Carbon monoxide difference assay at 444 nm yielded a concentration of 1.98µM for active protein which was significantly less than the concentration of absolute protein yield. Figure 28 below shows electrophoretic gel of the 1.98µM active protein concentration.

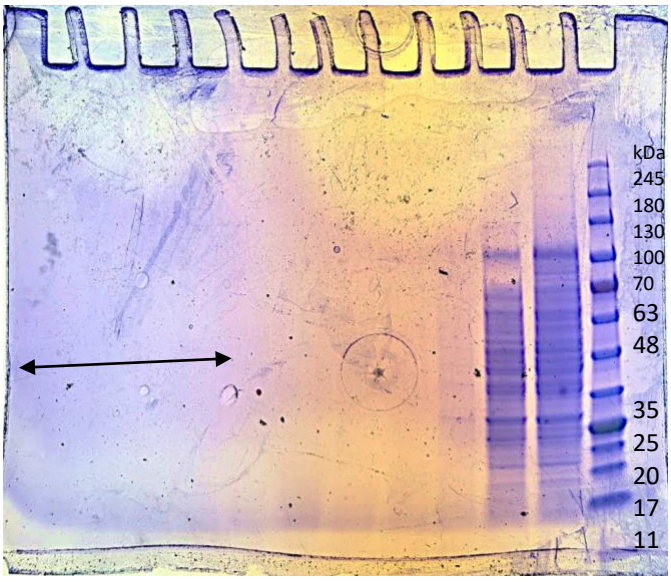

Figure 28: Electrophoretic gel of 1.98µM pET28a CYP4X1. Right to left electrophoretic gel bands showing protein ladder, Ni-NTA flowthrough, resuspension rinse, wash phase, CM flowthrough, CM wash, CM elution near 50 kDa from 1.9 µM pET28a.

3.1.15. The Fourteenth protein expression and purification. Experimental attempt yielded an excellent turbidity for starter culture and OD 600 of 0.95 before induction via ALA

and IPTG. 3ml of IPTG and ALA mixture was aliquot into 3 liter of terrific broth and incubated at 180rpm at 32c for 3 days. Harvested cells by emptying grown cells in eight 400ml containers. Pelletized bacterial cells exhibited the requisite heme thiolate brick red coloration. I carried out membrane protein extraction using Cymal-5 and centrifuged extracted protein at 19000 rpm for 20 minutes then the lysate was separated for chromatographic purification. Results from purification was negatively impacted by protein precipitation on the Ni-NTA column. However, a significant proportion of the target protein was obtained in the wash phase and no ion exchange purification was conducted. Concentration of protein obtained after carbon monoxide difference assay was practically nonexistent at -22.5μM. Thus, making it unsuitable for binding affinity and crystal screening.

3.1.16 The fifteenth protein expression and purification. This experimental attempt was carried out using a pET28a vector. 100μL of CYP4X1 glycerol stock was inoculated into LB media and incubated overnight. The resultant starter culture obtained yielded sufficient turbidity. Starter culture was aliquot in 3 liters of terrific broth for scaled up growth. Ensured OD_{600} was 1.423 before induction for scaled up growth with IPTG and ALA. Scaled up E. coli cells were harvested, lysed open through sonication to access membrane protein. This was followed by protein extraction using Cymal-5 and CHAPS detergents for 1 hour on an ice bath. Extracted protein was centrifuged at 19000 rpm for 20 mins. The supernatant which represents the lysate was kept for chromatographic purification. The affinity column results were affected by a significant drop in pH of the elution buffer used. The buffer used dropped pH due to its age in storage. Absolute protein spectrum of wash phase eluate in Figure 29 yielded characteristic peaks near 400 and 280 nm respectively. However, the peaks did not illustrate optimum purity in a 1:1 fashion and as seen earlier in the project with the pCW4X1 combination. Concentration

calculated from obtained absorbance near 400nm was 5.59µM while the spectrum from carbon monoxide difference assay for active protein obtained in Figure 30 was very low at 0.05µM. No further protein concentration or characterizations were carried out.

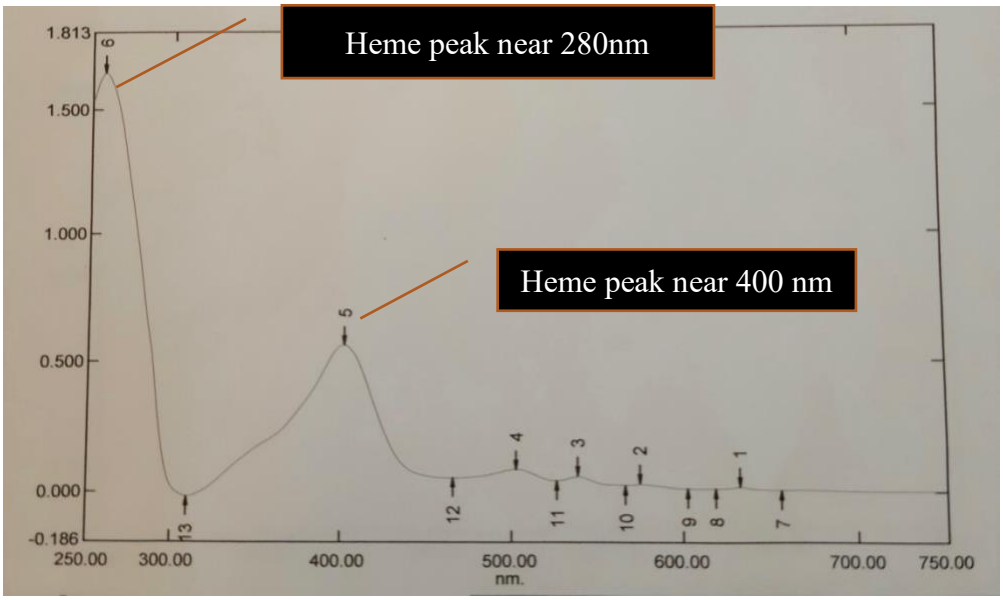

Figure 29: Absolute protein spectrum from pET28a CYP4X1.

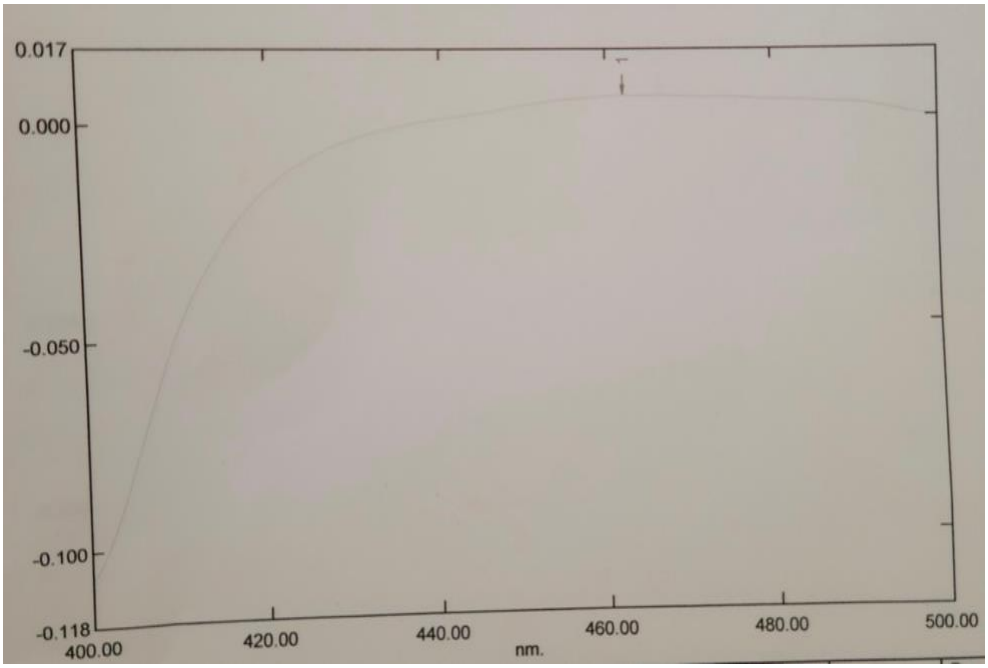

Figure 30: Carbon monoxide difference assay from pET28a CYP4X1.

The protein used for binding assays was obtained from experiments by a fellow graduate student Mehwish Khokhar whom in collaboration with Dr DeVore successfully obtained an optimum purified protein elution for the target membrane protein prior to binding affinity assays. As evident in Figure 31. SDS-PAGE was conducted on the lysate elution obtained from that experiment to ascertain purity.

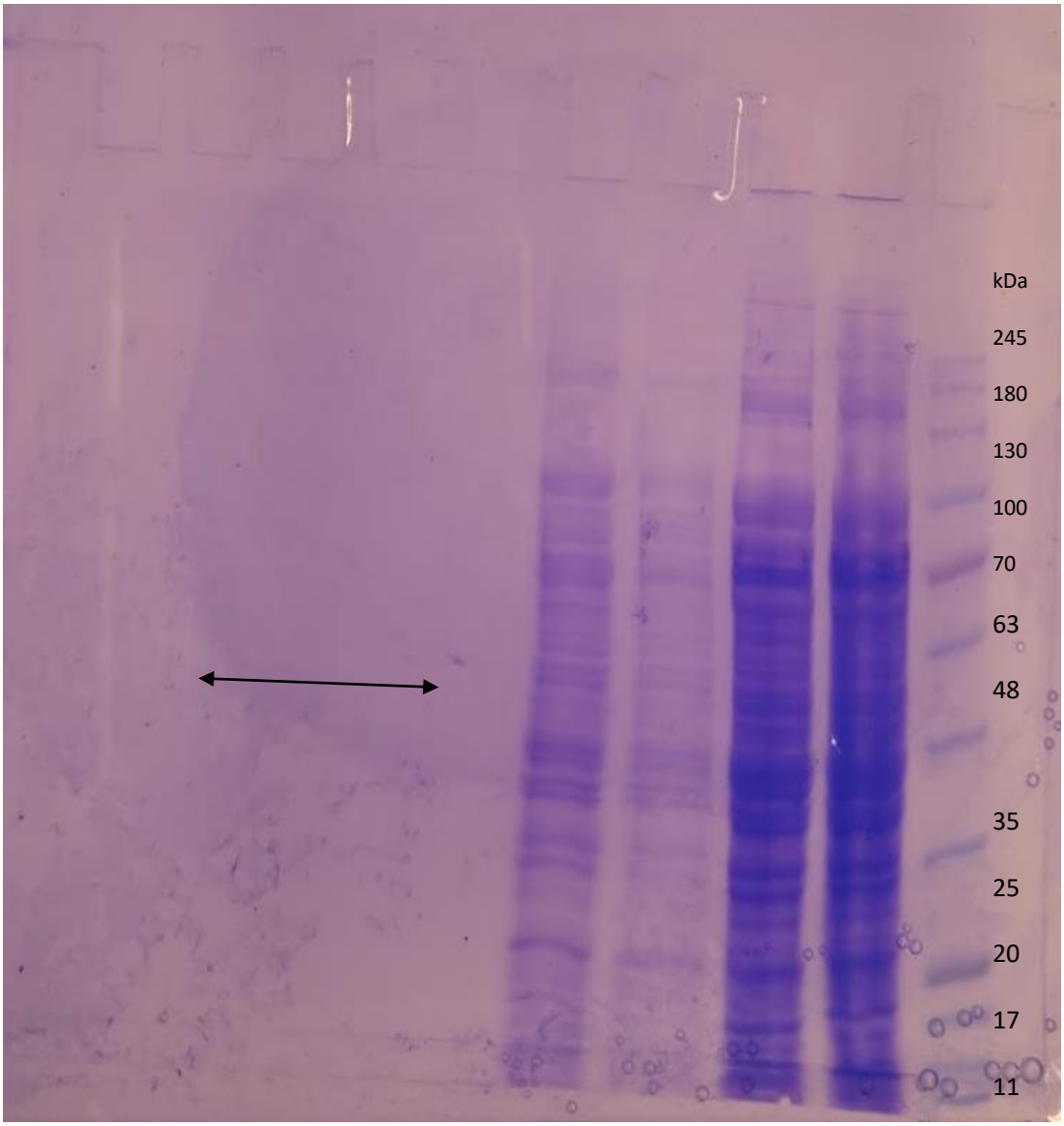

Figure 31: Electrophoretic gel of successful 4.1mM CYP4X1. Right to left protein ladder, flowthrough, resuspension rinsate, wash phase and elution near 50 kDa from 4.1µM pET28a Ni-NTA purified protein obtained by Mehwish Khokhar and Dr DeVore's purification endeavors.

The bands near 50kDa looks unclean with multiple bands indicating the presence of other proteins present. However, the presence of bands near 50kDa corroborates the presence of CYP450 protein irrespective of concentration.

3.2 Substrate Binding Affinity Assays

Binding assays of potentially favorable compounds was conducted to test their affinity for CYP4X1 protein. The end goal was to determine binding constants of known and unknown substrates. The binding assays were conducted on 4.1µM CYP4X1 protein Ni-NTA elution obtained from efforts by Mehwish Khokhar and Dr Natasha DeVore. This prep was purified using Cymal-5 and tris buffers.

Obtaining substrates binding affinity results starts with a series of stoichiometric calculations; this is needed to determine the applicable protein and ligand stock concentrations required for the assay. A stepwise example is as follows:

Anandamide stock for 750µL cuvette volume:

For 1µM of CYP4X1:

(4.1µM) x (ZµL) = (1µM) x (750µL). Therefore, ZµL = 182.9µL.

So 182.9µL of purified CYP4X1 lysate is aliquot into 567.1 µL of elution buffer.

Anandamide stock (M.W 347.53g/mol)

10mg in 200µL of anandamide

10mg/200µL = 0.01g/0.0002L = 50g/L

Molarity = (50g/L) / (347.53g/mol) = 0.144 mol/L = 0.144 M = 144 mM.

For 1mM Anandamide Stock:

(1mM x 1 ml) / 144mM = 0.0069 ml = 6.9µL

So 6.9µL of 1mM anandamide stock was aliquot into 993.1µL of ethanol.

For 0.5mM Anandamide Stock:

500µL of 1mM anandamide stock was aliquot into 500µL of ethanol. After the above calculation, binding affinity assays were carried out by aliquoting 750µL of 1µM CYP4X1 into a pair of UV-VIS cuvette. UV-VIS wavelength scan is set from 500nm – 350nm range. Then ligand stock volume additions are calculated and added to the cuvette in a stepwise fashion as shown below. Same calculated amount of 100% ethanol is also added to the reference cuvette. For the assay, the UV-VIS spectrophotometer is used in a dual beam mode, where an equal amount of ethanol is added to the reference cuvette and ligand is added to the sample cuvette.

Additions:

For 0.5µM increment; (0.5 µM x 750µL) = (500µM x ZµL); X = 0.750µL

For 1µM increment; (0.5µM x 750.75µL) = (500µM x ZµL); X = 0.751µL

For 2 µM increment; (1µM x 751.501µL) = (1000µM x ZµL); X = 1.50µL

There is a 7-minute wait time after every stock and ethanol addition before scanning for absorbance. The volume addition of ligand stock goes on till the targeted molarity is reached. Binding affinity assays were carried out for the following compounds arachidonic acid, anandamide, ketoconazole, eicosapentaenoic acid, phenethyl isothiocyanate (PEITC) and the results were as follows:

3.2.1 Arachidonic acid. Arachidonic acid has been reported to be a substrate of CYP4X1. As a substrate, the binding spectrum shifts should ideally yield a soret peak at a maximum wavelength of type 1 spectral shift (390 – 405 nm) and trough at 415 - 420 nm. (Ortiz de Montellano, 2015). Binding assays of CYP4X1 with arachidonic acid was tried a total of four

times with their spectral peaks and troughs shifts shown in Figure 32. Each time, the shifts were inconsistent with what was expected from a published substrate.

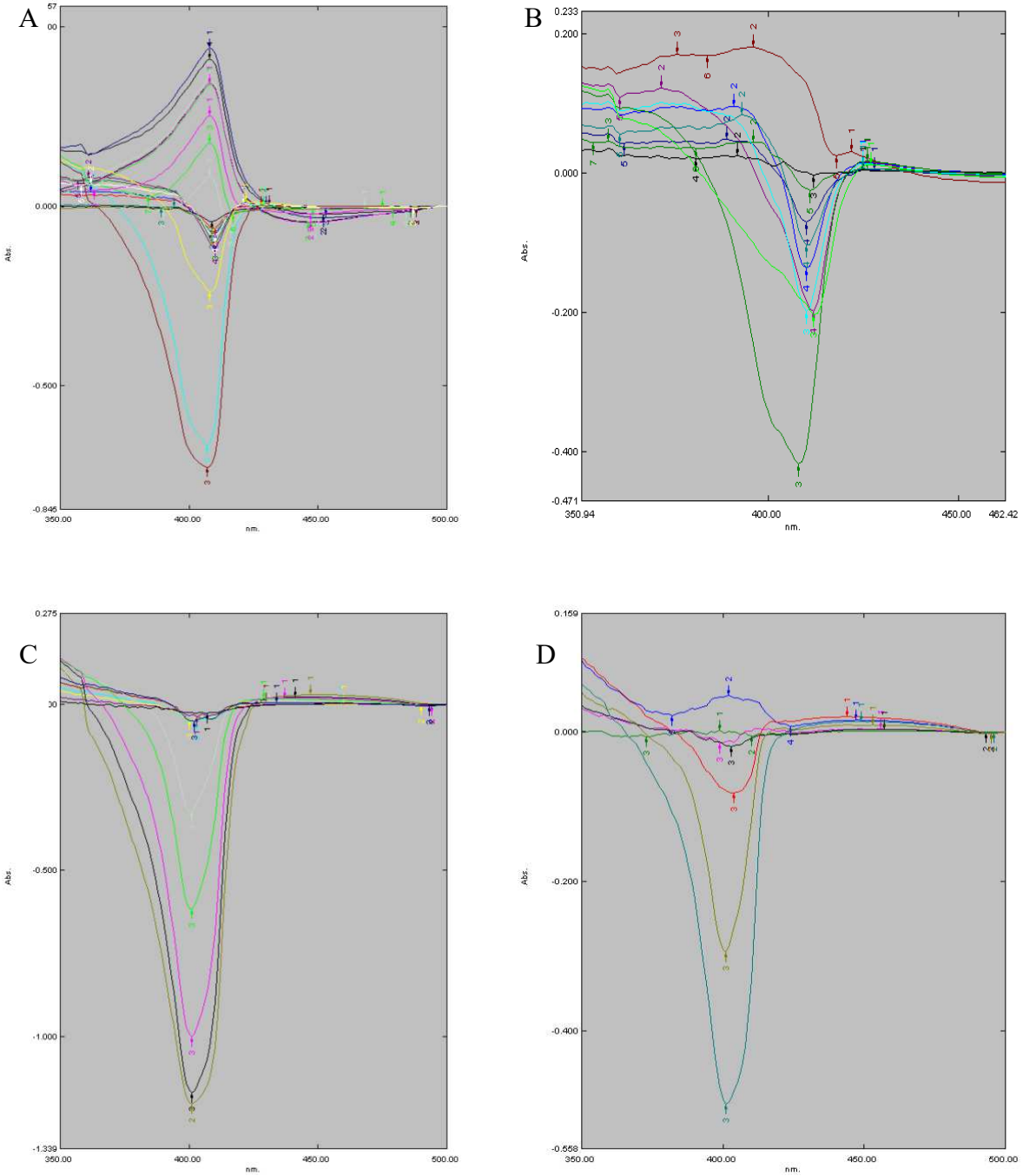

Figure 32: Spectrum of arachidonic acid binding assays. Top left to bottom right showing spectra images of peaks and troughs of arachidonic acid binding assay attempt A-D.

Although none of these assays have the absorbance shifts expected for a literature reported substrate; However, the saturation curve plots were fitted according to the peak or trough present and plotted against the concentration of arachidonic acid added. Overall, Absorbance versus concentration data points does not fit the expected binding saturation curve due to poor quality. However, the curve trend is sigmoidal (S-shaped) and translates to the moderate (cooperative) binding of arachidonic acid to the protein. See Figure 33 for summary of binding saturation curves.

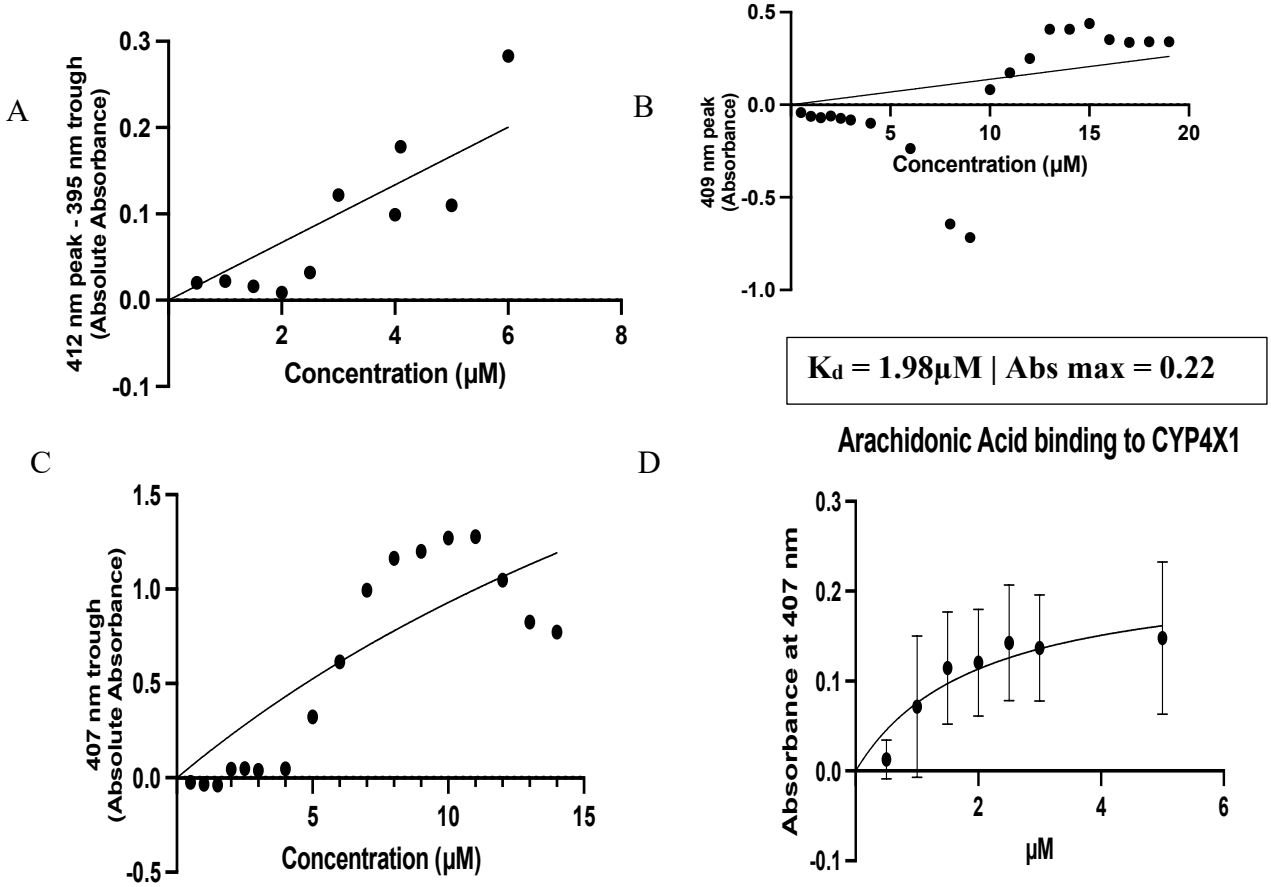

Figure 33. A) Saturation curve plot for the first arachidonic binding assay. B) Saturation curve plot for the third arachidonic acid binding assay. C) Saturation curve plot for the fourth arachidonic acid binding assay. D) The absorbance value at 407 nm from trials 1, 3, and 4 that were obtained at the same concentrations were averaged and plotted with standard deviation shown as error bars. Concentration data points that were only measured in trial 2 were excluded. The Kd is 1.98 μM arachidonic acid and the absorbance max is 0.2256. Overall, the average plot does not fit due to poor quality of substrate binding.

3.2.2 Anandamide Binding Assay. Saturation curve and spectra image shown respectively in Figure 34 and 35 below. Curve plot data clearly indicates no real ligand binding for the endogenous cannabinoid.

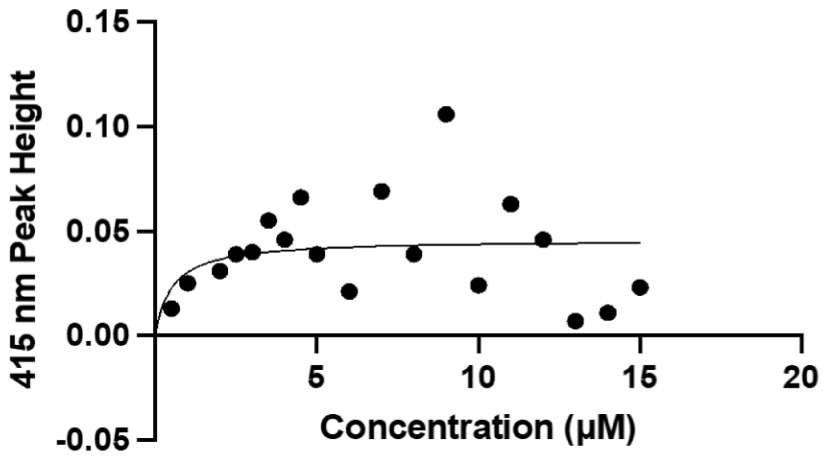

Figure 34: Saturation curve plot for anandamide binding assay

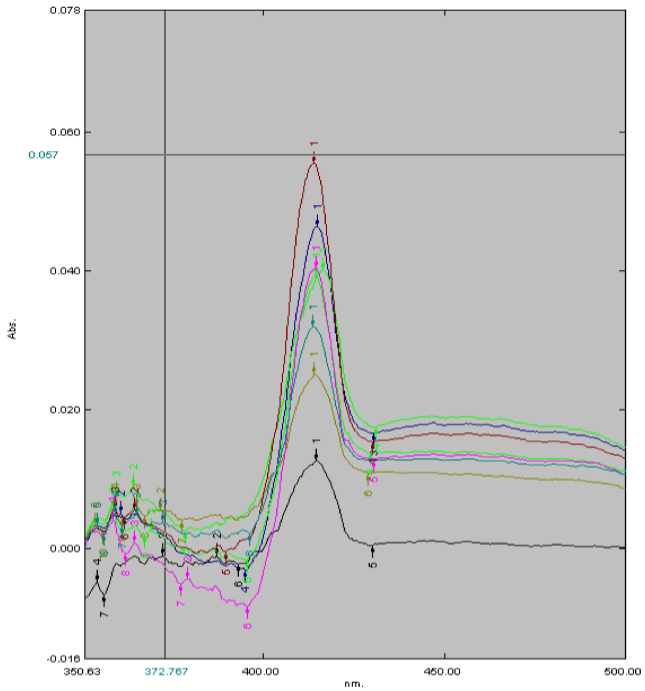

Figure 35: Spectrum of anandamide binding assay.

3.2.2 Ketoconazole Binding Assay. The ketoconazole binding affinity assay attempt yielded experimentally useful data with moderate quality of ligand binding in the second and third assay trials. The data obtained from the first trial cannot be plotted due to poor data quality. The data points in Figure 36 began from the origin and somewhat follows the expected binding saturation curve.

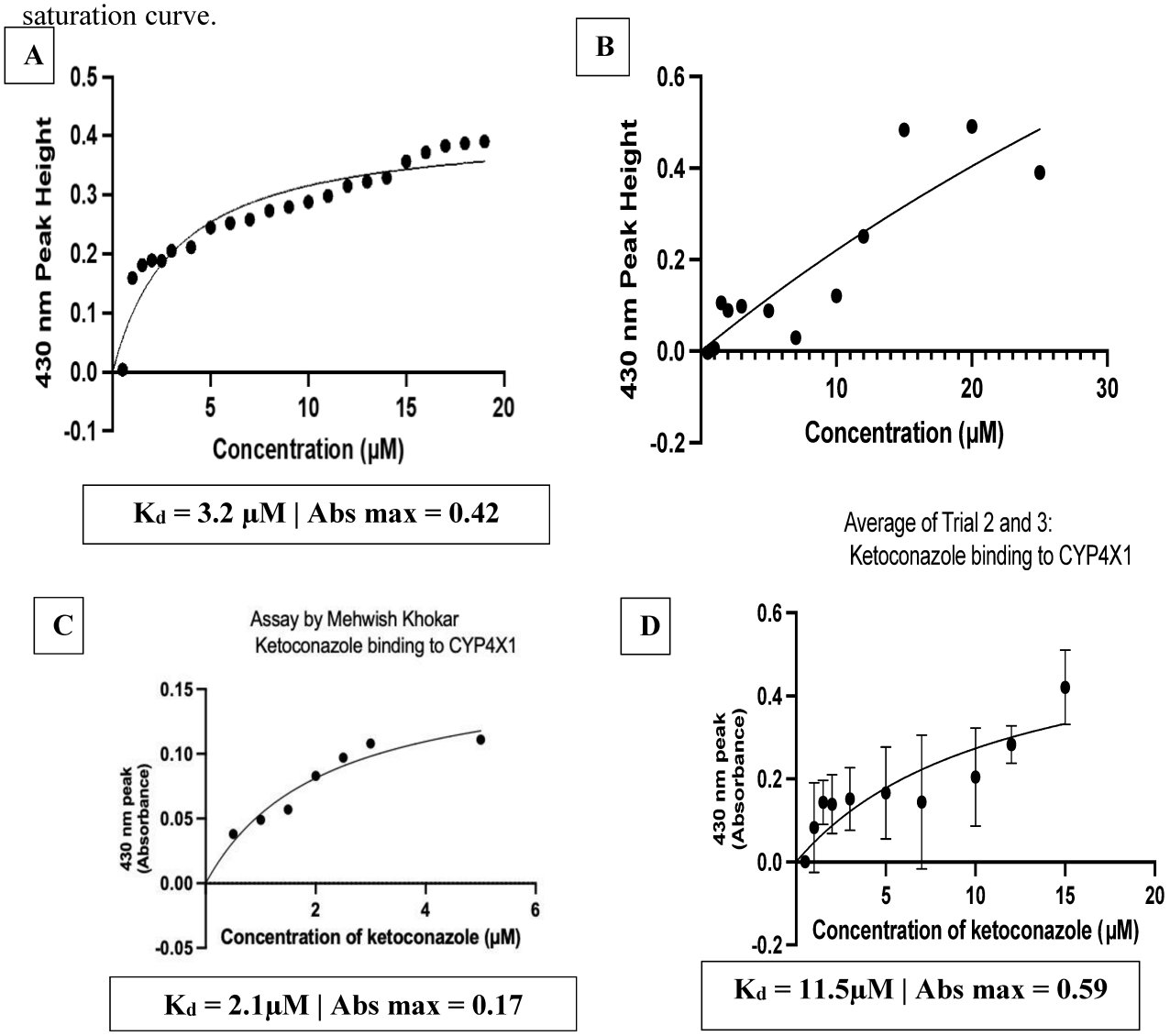

Figure 36. A) Trial 2 plotted by maximal absorbance at 30 nm. K_d is 3.2 μM ketoconazole and Absorbance max is 0.42 B) Trial 3 plotted by maximal absorbance at 430 nm. This data could not be fit by our nonlinear analysis under a one-substrate binding parameter. C) This assay was completed by Mehwish Khokhar with the same protein. K_d is 2.1 μM ketoconazole and absorbance max is 0.17 D) Trials 2, and 3 with maximal absorbance value at 430 nm and obtained at the same concentrations were averaged and plotted with standard deviation shown as error bars. Concentration data points measured in trial one was excluded. The K_d is 11.5 μM ketoconazole and the absorbance max is 0.59.

Using only peak heights, the saturation curve obtained was sigmoidal (S-shaped) while data obtained for the ketoconazole binding assay at maximal absorbance of 430nm yielded a dissociation constant (K_d) value of 3.22 µM for trial 2. Also, a K_d value of 11.5 µM upon average of trial 2 and 3 at similar concentrations. Interestingly, Mehwish Khokhar's binding assay obtained at a different concentration values yielded a dissociation constant value of 2.1µM. These results indicate moderate ketoconazole affinity to the protein.

However, it is crucial to note that the interpretation of dissociation constant value depends on what area of biochemical research focus is laid; for example, 1µM could be reported as high affinity in metabolism regulation or low in the design of antibodies. Figure 37 below shows spectrum with peaks and troughs from ketoconazole binding assay.

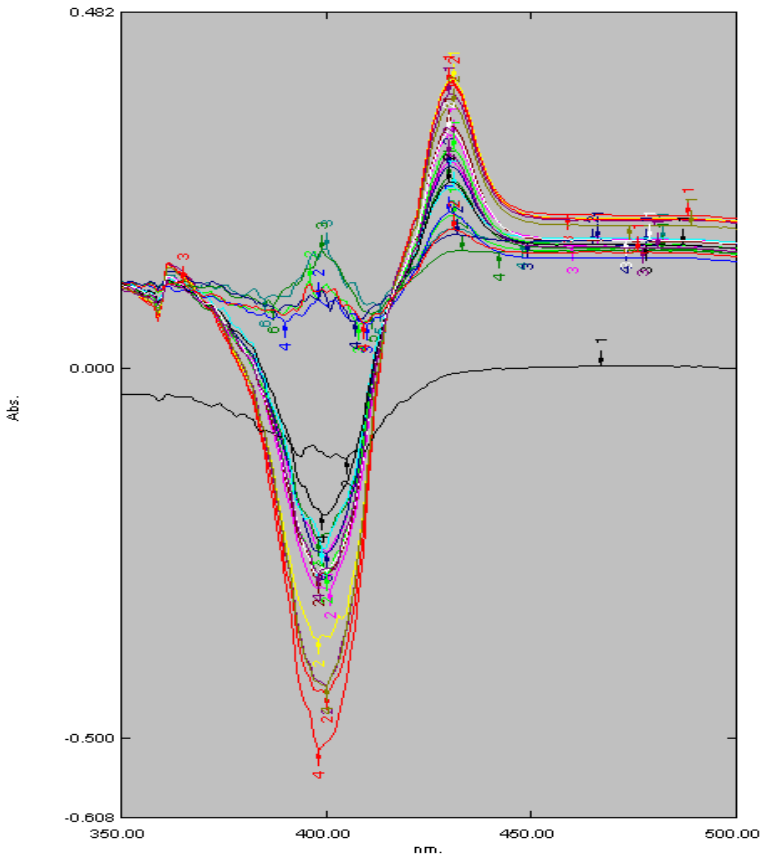

Figure 37: Spectrum of second ketoconazole binding assay.

3.2.3 Eicosapentaenoic Binding Assay. For eicosapentaenoic acid, obtained binding assay data shown in Figure 38 gave peaks and troughs with absorbance maximum at 400nm only This is indicative of the presence of free heme in solution. Substrate is clearly not binding to the protein.

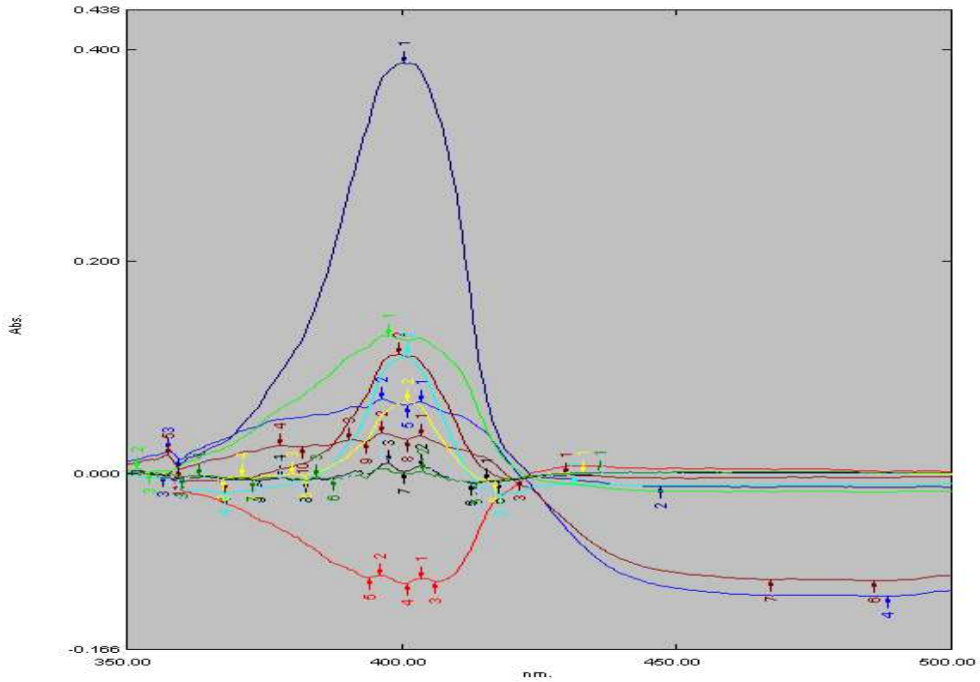

Figure 38: Spectrum of eicosapentenoic binding assay.

3.2.4 PEITC (Inhibitor) Binding Assay. Phenethyl isothiocyanate (PEITC) is an inhibitor with extensive (published) application in human cancer prevention. However, binding assay spectrum data obtained and shown in Figure 39 yielded unrecognizable sites of peak heights or trough for this potential inhibitor. The soret peaks and troughs at absorbance maximum obtained was at 465nm and 400nm wavelength respectively. The binding spectrum shifts should ideally yield a soret peak at a maximum wavelength of 425 nm – 435 nm and trough at 390 - 405 nm (Ortiz de Montellano, 2015).

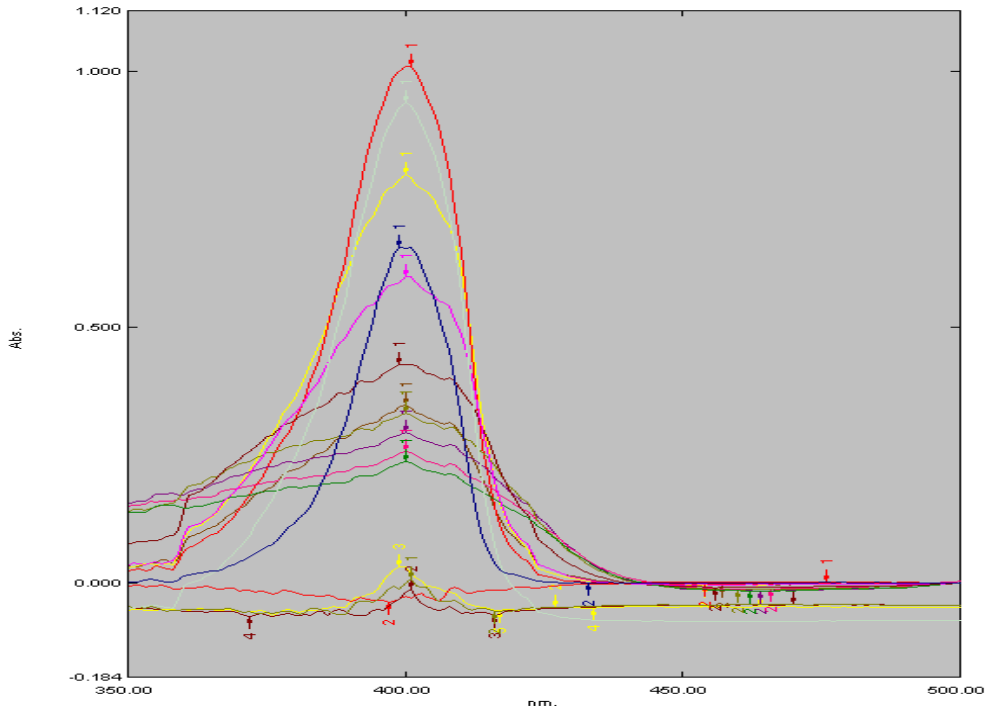

Figure 39: Spectrum of PEITC binding assay.

3.3 Crystal screening for setups

Crystal screening was made from the concentrated 160µM purified protein obtained from the twelfth CYP4X1 Protein Expression and purification experiment. Obtained image represents initial crystals hits from *commercial* screens which is an indicative milestone and a guide for future crystal optimization. Well B-12 from screening plates showed great potential with dark spots that could lead to crystals observed under the microscope as shown in Figure 40.

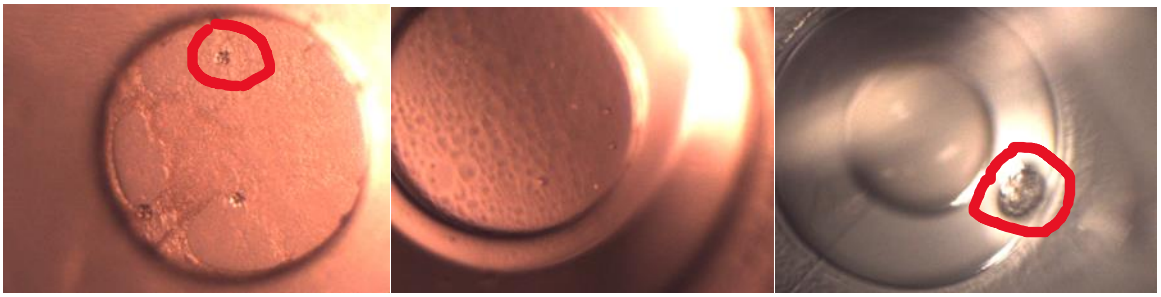
Figure 40: Crystals of CYP4X1.

CHAPTER 4 - DISCUSSION AND CONCLUSION

4.1 Discussion

The goal for this project as mentioned in the experimental design was to express the CYP4X1 gene in *E. coli* JM109 cell using either pCW or pET28a vector. Purifying the resulting protein and characterizing it primarily via substrate binding affinity assays. Lastly, a crystal screen is performed to determine the crystallization condition of CYP4X1 after the protein is optimally purified. Further optimization will be required in future experiments on this project before 3-D structure can be considered and obtained via X-ray crystallography.

Glycerol stock from previous research endeavors and from a new gene construct was mostly used to initiate experimental protocol on this project. Occasional cell transformation on culture plates was required particularly when using pCW vector. Application of antibiotic stock solution was an effective way to ensure the growth of targeted cells after cell transformation; as *E. coli* Jm109 cells transformed via pET28a were designed to be immune to kanamycin sulfate while cells transformed via pCW vector were designed to be immune to ampicillin during gene construct. Overall, *E. coli* Jm109 cells showed excellent turbidity after inoculation irrespective of what vector system was used, provided the right antibiotic stock was applied. This is an excellent sign of *E. coli* Jm109 cell growth.

Evaluation of CYP4X1 over the course of 15 protein expression attempts showed that when compared to pCW, the pET vector system delivered on a better yield in terms of concentration of active protein and signature heme thiolate brick red coloration, it was also the most adopted (11 times) in experimental trials. because from earlier data, it was the better of t2-vector system implemented for the cloning and expression of my recombinant protein in

E. coli. Consistent coffee brown coloration of harvested cells upon protein expression using pCW demonstrated lack of optimum efficacy of that vector; especially in the expression of the functionally pivotal heme-thiolate prosthetic group.

Obtaining purified and significant molar concentration of CYP4X1 protein from expression endeavors was critically important prior to characterization; but the experimental outcomes delivered a shortfall in reaching this objective. However, failed attempts, successes, vectors used, issues encountered, corrections and tweaks made in CYP4X1 protein expression is summarized in Table 2.

Table 2: Summary of protein expressions and purifications.

Attempt	Vector	Expression and/or Assay Results	SDS-PAGE Outcome	Purification Observation	Corrections
First	pET28a	UV-VIS analysis yielded a 400 nm heme peak. However, soret peak near 280nm was saturated upon protein assay	Coomassie stained gel gave multiple horizontal bands near 50kDa upon SDS-PAGE	Protein eluted from cobalt column matrix in the wash phase	Use LP Bio-Rad autosampler and fraction collector instead of gravity for purifications
Second	pET28a	Soret peaks obtained via UV-VIS analysis indicate suboptimal yield for CYP4X1. judging by 280nm and 410nm peak ratio upon protein assay	No identifiable single bands near 50kDa	Protein eluted from cobalt column matrix mostly in the wash phase and some in the elution	Vector was changed to pCW
Third	pCW	Coffee brown coloration of bacterial cell pellets indicates poor expression of the heme-thiolate prosthetic group. Obtained protein absorbance was not workable due to an unrecognized elevated spectral shift.	No identifiable single bands near 50kDa	Protein eluted from cobalt column matrix in the wash phase	Ensured optimal OD600 between 0.4 -1.2 from here on out and repeated experiment with the same protocol Nil

Table 2, Continued.

Attempt	Vector	Expression and/or Assay Results	SDS-PAGE Outcome	Purification Observation	Corrections
Fourth	pCW	Coffee brown color persists of bacterial pellets persists, but protein assay yielded spectrum with 1:1 soret peak ratio near 410 nm and 280nm respectively. Indicating good yield.	Positive single horizontal bands obtained near 50kDa	Protein was purer due to the addition of ion-exchange column	Nil
Fifth	pCW	Coffee-brown coloration of bacterial cell pellets persists. Protein concentration was too low despite good yield.	Positive single bands obtained near 50kDa	Protein was purer due to the addition of ion-exchange column	Return to pET28a vector and Ni-NTA beads for purification
Sixth	pET28a	Protein concentration from Ni-NTA rinsate was at 22.8µM after assay. Carbon monoxide difference assay did not yield active protein.	Nil	CYP4X1 did not make it to the wash phase as protein did not bind well to the Ni-NTA column	Repeat the sixth experimental protocol
Seventh	pET28a	Protein concentration from Ni-NTA column elution was at 25.54 mM after assay. However, the protein was not of optimum yield evident by the peak around 280nm being saturated. Concentration of active protein after CO difference assay was 1.42µM	SDS-PAGE gel was unusable with untraceable bands	Lysate crashed on the Ni-NTA column. Significant protein came off the Ni-NTA column in the wash phase. Attempts to elute purified protein with increased concentration of imidazole concentration yielded no positive outcome. Wash phase was subjected to additional CM (ion exchange) purification.	Marked increase in prepared growth media (terrific broth) used; from 2 liters to 3 Liters from here on out. The idea was to significantly increase the amount of obtainable transformed E. Coli cells upon harvest. Also, instead of tris buffers which were used on all purifications before this one, phosphate-based buffers were used.
Eight	pET28a	Protein concentration obtained from assay after Ni-NTA eluates (wash plus elution) was 6.12µM.	Gel disintegrated during Coomassie solution staining. Bands barely show any protein of interest. No identifiable single bands near 50kDa	Protein loaded well with lysate forming a decent ring around the affinity column. Data obtained from collected fractions showed that most of the target protein came off in the wash phase.	Cymal-5 detergent was combined with for membrane protein extraction. Unlike previous expression and purification protocol that used CHAPS only.

Table 2, Continued.

Attempt	Vector	Expression and/or Assay Results	SDS-PAGE Outcome	Purification Observation	Corrections
Ninth	pET28a	Triton and CHAPS detergent was used for protein extraction. Detergent combination yielded the best lysate obtained thus far. Concentration of protein obtained after assay was 6.12μM which is too slow. Even before assay for active protein is carried out	Nil	Unfortunately, Lysate did not bind well to the Ni-NTA column despite being the most visible consistent brick-red coloration obtained	Triton X-100 and CHAPS detergent were used during membrane protein extraction and solubilization.
Tenth	pET28a	CHAPS and Cymal used for protein extraction	Nil	Protein precipitated on the NiNTA column	Cymal-5 and CHAPS detergent were used during membrane protein extraction.
Eleventh	pCW	Impure and low concentration of purified protein which was too low for characterization	Multiple horizontal bands near 50kDa upon Coomassie stained gel inspection.	Protein eluted from NiNTA column in the wash phase fractions.	A return to Triton X-100 and CHAPS detergent combination for membrane protein extraction and solubilization
Twelfth	pET28a	Purified protein concentration was too low for binding assays but yielded crystal hits in well B12.	Nil	Protein eluted from NiNTA column in the wash phase fractions.	Used Cymal-5 Only as detergent for extraction and solubilization. Returned to pET28a vector
Thirteenth	pET28a	Concentration of active protein was1.98μM which is lower than the 4.1μM eventually used for binding assays.	Multiple horizontal bands near 50kDa upon Coomassie stained gel inspection.	Protein precipitated on the NiNTA column	No Change in Experimental Protocol
Fourteenth	pET28a	Nonexistent active protein after CO difference assay.	Nil	Protein precipitated on the NiNTA column	No Change in Experimental Protocol
Fifteenth	pET28a	Concentration of absolute protein was 5.59μM after assay. Active protein concentration obtained (0.05μM) after CO difference assay was too low. Not suitable for binding assays.	Nil	Protein eluted from NiNTA column in the wash phase fractions.	No Change in Experimental Protocol

After obtaining optimal protein yield was binding assay. Binding assays of potentially favorable compounds like arachidonic acid, anandamide, ketoconazole, eicosapentaenoic and PEITC were conducted to test their affinity on CYP4X1 protein and to determine which compound from the available group of substrates have the potential for protein active site target. A 4.1μM CYP4X1 protein obtained from Mehwish Khokhar's purification attempt was assessed for purity via SDS-PAGE and utilized for binding assays.

For arachidonic acid, the trend of absorbance against concentration showed moderate binding to the CYP4X1 protein judging by the average saturation curve with a dissociation constant, K_d value of 1.98μM (Figure 33, Section D). For anandamide, the compound shows no real ligand binding for this endogenous cannabinoid (Figure 34).

For ketoconazole however, the results obtained for the second set of binding assays indicated moderate ligand affinity to the CYP4X1 protein. The data points somewhat follow the saturation curve with a dissociation constant (Kd) value of 3.22 μM when incorporating only peak heights and 9.06 μM upon absolute difference between peaks and troughs. Ideally, the lower the Kd value, the better the substrate binding potential. The Kd value quantifies the equilibrium between the free ligand in solution and binding to a site in the protein (Figure 36).

For eicosapentaenoic acid binding assay, the data obtained gave peaks and troughs with absorbance maximum at 400nm. This is indicative of the presence of free heme in solution; Thus, the substrate is clearly not binding to the actual protein (Figure 38). For PEITC (Inhibitor) binding assay, the soret peaks and troughs at absorbance maximum obtained were at 465nm and 400nm wavelength respectively. However, binding assay data obtained yielded unrecognizable sites of peak heights or trough for this potential inhibitor (Figure 39).

4.2 Conclusion

A total of fifteen protein expression and purification protocols were conducted to obtain enough concentration to characterize the CYP4X1 protein via a series of binding affinity assays and crystal structure determination. CYP4X1 gene were expressed successfully in *E. coli* using pET28a and pCW vectors. Results obtained from expression attempts showed that pET28a vector yielded more functional CYP4X1 protein evident by the appearance of heme thiolate coloration and a series of much better CYP4X1 protein concentration yields.

In the thirteenth trial of protein expression and purification experiments, a 1.98 μM active CYP4X1 protein was obtained via pET28a vector. Albeit it was a 0.24 μM active CYP4X1 protein obtained in the twelfth experimental trial (also via pET28a vector) that resulted in dark spots and crystal hits during a commercial screening for crystallization conditions with further optimizations required. However, the volume of both the 1.98μM and 0.24 μM active CYP4X1 protein was just too low for substrate binding assays.

Eventually, an optimally purified and metabolically active 4.1μM CYP4X1 from a research associate's experiment was eventually used for substrate binding assays due to the better yield quality. The binding assay of substrates do not tell us about the functional active sites of the target protein but rather gives an indication of the potential for certain biologically favorable compounds and their analogs to affix suitably. Thus, giving guidance for future characterization methods that could lead to active sites discovery of the three-dimensional structure of the protein. Amongst the range of compounds assayed, arachidonic acid and ketoconazole have demonstrated to be relatively cooperative compounds yet with moderate substrate binding to the CYP4X1 protein. This conclusion was reached using dissociation constants (from prism 8 software) obtained from average absorbance values of multiple trials at

similar concentrations and plotted with standard deviation shown as error bars. Substrates like arachidonic acid and ketoconazole with their Kd values clearly indicates the cooperative tendency of these molecules to bind to the CYP4X1 protein. Same protein which now has a crystal hit from the initial screening conditions (Figure 40).

Future work on this project may attempt to optimize the purity of the CYP4X1 protein yield before characterization via a methodology that incorporates ketoconazole in the purification buffers alongside Cymal-5 because it's a good inhibitor. Alternatively, dialysis technique can be adopted to reduce the impact of imidazole or to use alternatives to imidazole found in literature. Imidazole has been reported to adversely influence crystallographic studies and metabolic assays (Van Vugt-Van der Toorn, Dixon, & Vervoort, 2001). Lastly, other substates may be tried for binding assays with purified CYP4X1.

REFERENCES

Al-Anizy, M., Horley, N., Kuo, C., Gillett, L., Laughton, C., Kendall, D., Barrett, D., Parker, T., & Bell, D. (2006). Cytochrome P450 Cyp4x1 is a major P450 protein in mouse brain. *The Federation of European Biochemical Societies Journal, 273*(5), 1-12.

Bylund, J., Zhang, C., & Harder, D. (2002). Identification of a novel Cytochrome P450, CYP4X1, with unique localization specific to the brain. *Biochemical and Biophysical Research Communications, 296*(3), 677-684.

Carmeliet, P., & Jain, R. (2011). Principles and mechanisms of vessel normalization for cancer and other angiogenic diseases. *Natural Reviews Drug Discovery,* 10, 417-427.

Carver, K., Lourim, D., Tryba, A., & Harder, D. (2014). Rhythmic expression of CYP450 epoxygenases CYP4X1 and CYP2C11 in the rat brain and vasculature. *American Journal of Physiology, 307*(11), C989-C998.

Cristino, L., Becker, T., & DiMarzo, V. (2014). Endocannabinoids and energy homeostasis: An update. *Biofactors, 40*(4), 389-397.

Davis, C., Liu, X., & Alkayed, N. (2017). Cytochrome P450 eicosanoids in cerebrovascular function and disease. *Pharmacology and Therapeutics,* 179, 31-46.

Dong, L., Zou, H., Yuan, C., Hong, Y. H., Kuklev, D. V., & Smith, W. L. (2016). Different Fatty Acids Compete with Arachidonic Acid for Binding to the Allosteric or Catalytic Subunits of Cyclooxygenases to Regulate Prostanoid Synthesis. *The Journal of Biological Chemistry*, *291*(8), 4069–4078.

Hsu, M., Savas, U., Griffin, K., & Johnson, E. (2007). Human cytochrome P450 family 4 enzymes: function, genetic variation, and regulation. *Drug Metabolism Reviews, 39*(2), 515-538.

Kalsotra, A., & Strobel, H. (2006). Cytochrome P450 4F subfamily: at the crossroads of eicosanoid and drug metabolism. *Pharmacological Therapeutics, 112*(3), 589-611.

Kirschian, N., & Wilson, J. (2012). Phylogenetic and functional analyses of the CYP450 family 4. *Molecular Phylogenetics and Evolution, 62*(1), 458-471.

Kumar, S. (2015). Computational identification and binding analysis of orphan human cytochrome P450 4X1 enzyme with substrates. *BMC Research Notes,* 8, 9.

Kharkwal, H., Batool, F., Koentgen, F., Bell, D. R., Kendall, D. A., Ebling, F., & Duce, I. R. (2017). Generation and phenotypic characterization of a cytochrome P450 4x1 knockout mouse. *PloS one*, *12*(12), e0187959. https://doi.org/10.1371/journal.pone.0187959

Murray, G., Patimalla, S., Stewart, K., Miller, L., & Heys, S. (2010). Profiling the expression of Cytochrome P450 in breast cancer. *Histopathology, 57*(2), 202–211. https://doi.org/10.1111/j.1365-2559.2010.03606.x

Ortiz de Montellano PR (Ed.) (2015) Cytochrome P450 Structure, Mechanism, and Biochemistry, Fourth, Springer International Publishing.

Pal, A., Metherel, A. H., Fiabane, L., Buddenbaum, N., Bazinet, R. P., & Shaikh, S. R. (2020). Do eicosapentaenoic acid and docosahexaenoic acid have the potential to compete against each other? *Nutrients*, *12*(12), 3718. https://doi.org/10.3390/nu12123718

Raynal, B., Lenormand, P., Baron, B., Hoos, S., & England, P. (2014). Quality assessment and optimization of purified protein samples: why and how? *Microbial Cell Factories*, *13*(1), 1-10.

Rosano, G. L., & Ceccarelli, E. A. (2014). Recombinant protein expression in Escherichia coli: advances and challenges. *Frontiers in Microbiology*, 5, 172.

Ross R. A. (2003). Anandamide and vanilloid TRPV1 receptors. *British Journal of Pharmacology*, *140*(5), 790–801.

Snider, N. T., Kornilov, A. M., Kent, U. M., & Hollenberg, P. F. (2007). Anandamide metabolism by human liver and kidney microsomal cytochrome P450 enzymes to form hydroxyeicosatetraenoic and epoxyeicosatrienoic acid ethanolamides. *Journal of Pharmacology and Experimental Therapeutics*, *321*(2), 590-597.

Stark, K., & Guengerich, F. (2007). Characterization of orphan human cytochromes P450. *Drug Metabolism Reviews, 39*(2), 627-637. https://doi.org/10.1080/03602530701467708

Stark, K., Dostalek, M., & Guengerich, P. (2008). Expression and purification of orphan cytochrome P450 4X1 and oxidation of anandamide, *The Federation of European Biochemical Societies Journal, 275*(14), 3706-3717.

Tallima, H., & El Ridi, R. (2018). Arachidonic acid: physiological roles and potential health benefits–a review. *Journal of Advanced Research*, 11, 33-41.

Van Vugt-Van der Toorn, H., Dixon, C. J., & Vervoort, J. R., (2001). A novel purification. Hefti, Mtion method for histidine-tagged proteins containing a thrombin cleavage site. *Analytical biochemistry*, *295*(2), 180–185. https://doi.org/10.1006/abio.2001.5214.

Wang, C., Li, Y., Chen, H., et al. (2018). CYP4X1 inhibition by flavonoid CH625 normalizes glioma vasculature through reprogramming TAMs via CB2 and EGFR-STAT3 axis. *Journal of Pharmacology and Experimental Therapeutics,* 365, 72-83.

Waskell, L., & Kim, J.J.P. (2015). Electron Transfer Partners of Cytochrome P450. In: P.R.O. de Montellano (Ed.), *Cytochrome P450: Structure, Mechanism, and Biochemistry* (4th Ed., pp. 33–68). Springer International Publishing.

Wooh, J. W., Kidd, R. D., Martin, J. L., & Kobe, B. (2003). Comparison of three commercial sparse-matrix crystallization screens. *Acta Crystallographica Section D: Biological Crystallography*, *59*(4), 769-772.